Quantification of Object Dynamics by Spatiotemporal Shape Analysis

Guido Gerig

James Fishbaugh

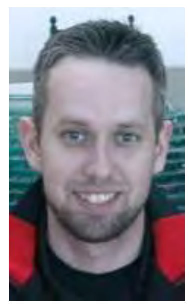

Marcel Prastawa

Scientific Computing and Imaging Institute,
University of Utah

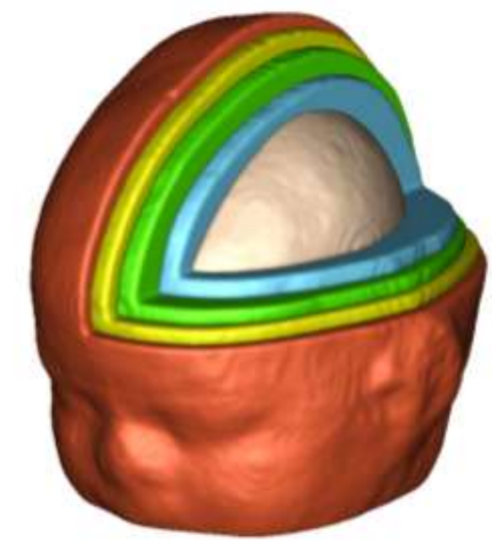

Stanley Durrleman, Xavier Pennec,
Nicholas Ayache, INRIA

THE BRAIN INSTITUTE
THE UNIVERSITY OF UTAH

SCI INSTITUTE

Longitudinal/Serial Image Data

Pediatrics: Brain Growth

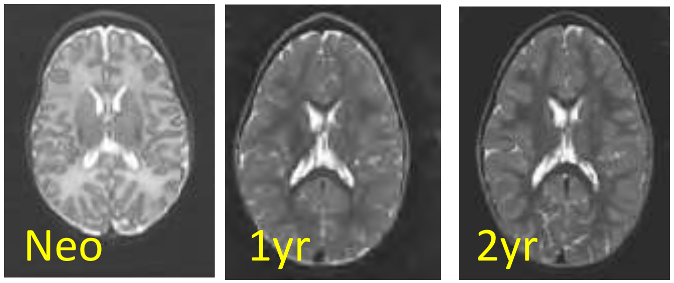

Aging / Neurodegeneration

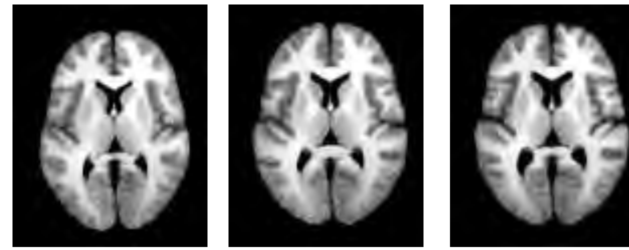

WM Maturation

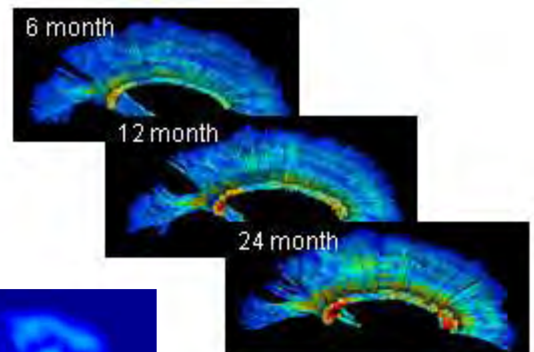

Tumor Growth

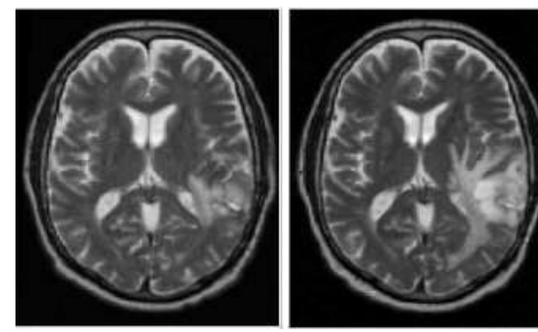

Trauma: Baseline – Follow-up

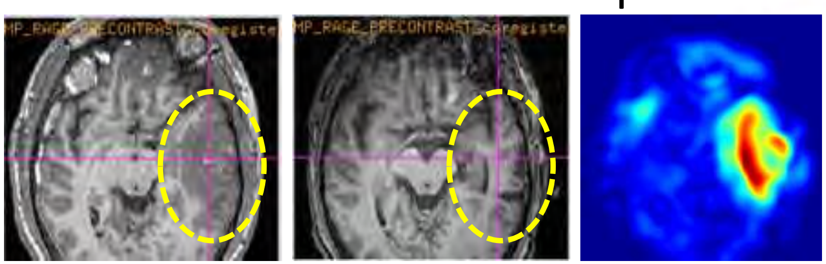

Jaw Growth 15-22 yrs

- Image analysis technology for 4D data is lagging behind acquisition
- Often: individual time-point analysis, ignores causality

Spatiotemporal Modeling: Natural Task in Clinical Reasoning

Motivation:

- Development, degeneration, effects of therapeutic intervention are dynamic processes.
- Personalized health care: Individual trajectories compared to expected “norm”.
- Clinical terminology: Atypical, Monitoring
  - Departure from typical development, deviation from healthy
  - Typical but delayed growth patterns, catch-up, atypical development
  - Analysis of recovery for each patient
  - Predict onset of clinical symptoms
  - Monitor efficacy of treatment

→ **Focus on longitudinal design & longitudinal analysis**

Shape Similarity in Twins

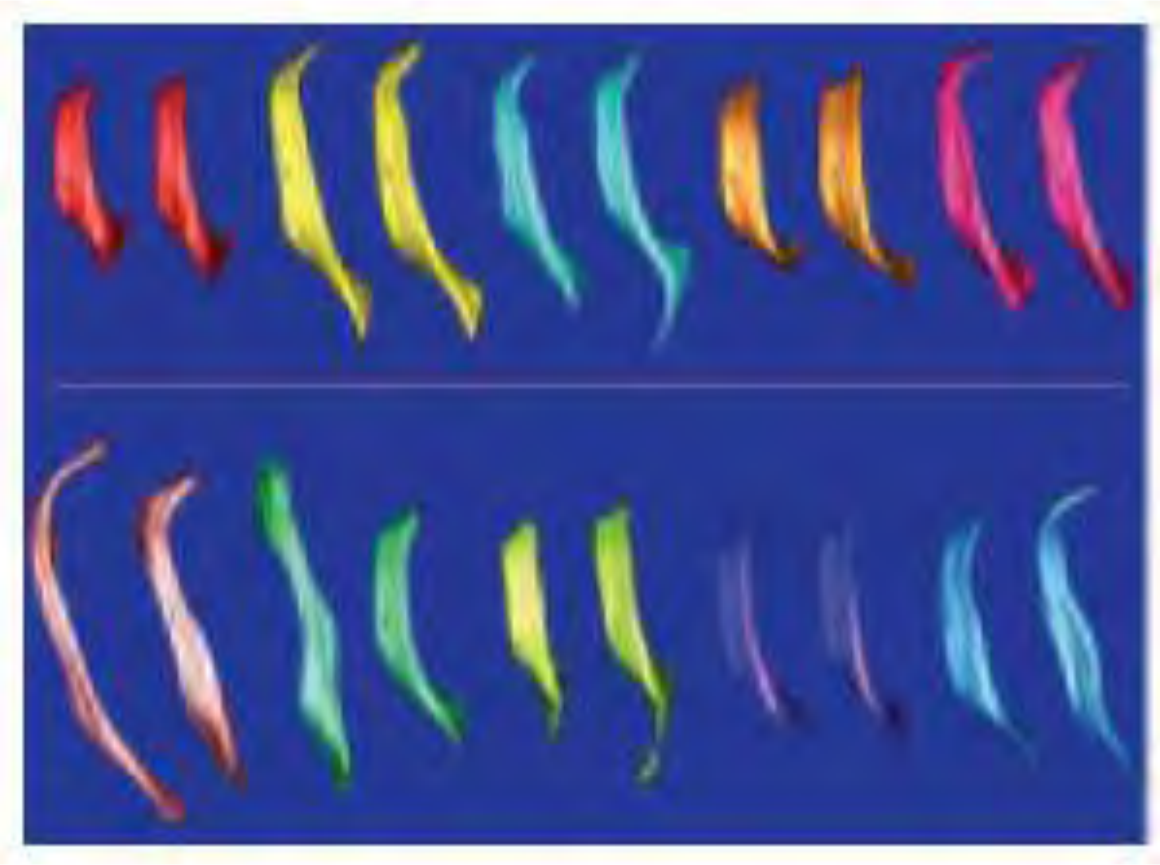

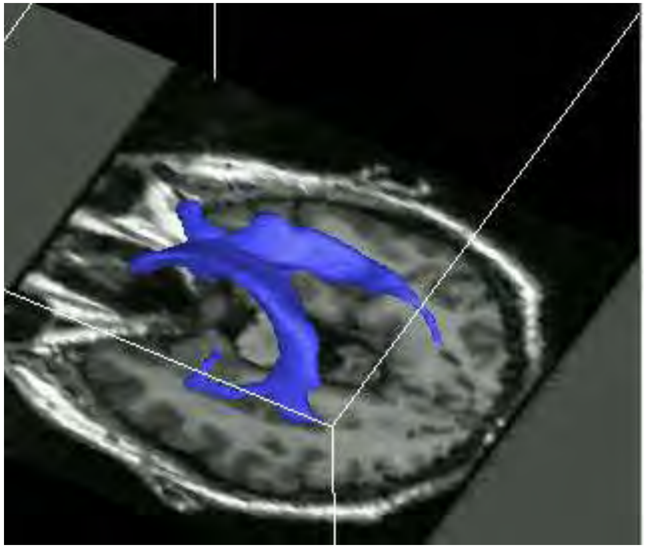

Upper row: identical twin pairs
Lower row: non-identical twin pairs

Styner/Gerig PNAS 2005

Shape >> Volume

Morphometric analysis of lateral ventricles in schizophrenia and healthy controls regarding genetic and disease-specific factors

Martin Styner*†‡§, Jeffrey A. Lieberman†¶, Robert K. McClure†‖, Daniel R. Weinberger**, Douglas W. Jones**, and Guido Gerig*†

*Department of Computer Science, University of North Carolina, Chapel Hill, NC 27599-3175; †Department of Psychiatry, University of North Carolina School of Medicine, Chapel Hill, NC 27599-3175; **Clinical Brain Disorder Branch, National Institute of Mental Health, National Institutes of Health, Bethesda, MD 20892; and §M. E. Müller Research Center for Orthopaedic Surgery, Institute for Surgical Technology and Biomechanics, University of Bern, CH-3014 Bern, Switzerland

Communicated by Frederick P. Brooks, Jr., University of North Carolina, Chapel Hill, NC, February 9, 2005 (received for review October 21, 2004)

Fig. 1. Graphical view of aligned and size-normalized ventricles. (*Left*) Superior view of left ventricles of five MZ twin pairs (*Upper*) and five DZ twin pairs (*Lower*) displayed from the top. Ventricles of co-twins are shown by using the same color. (*Right*) Sagittal view of right ventricles of 10 DS pairs, with affected and unaffected shown side by side. The third pair (*Upper Right*) was excluded because of hydrocephaly in the unaffected twin.

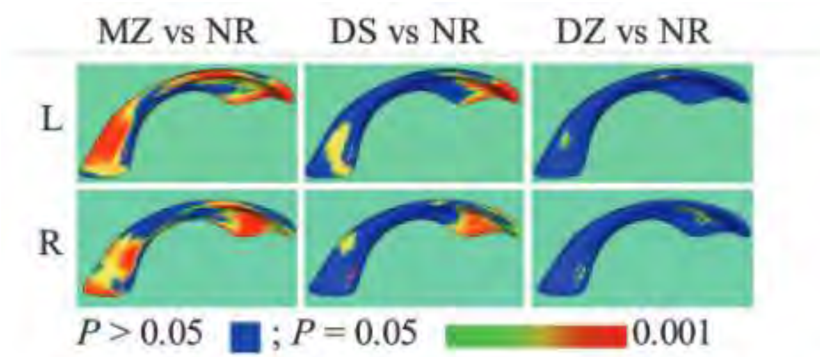

Fig. 6. Statistical maps displaying the locations of significant differences between groups for the co-twin analysis. The colors indicate the level of significance as shown in the color map. Results for group comparisons not shown in this figure did not have significant regions

Example Infant Study: Cross-sectional vs. Longitudinal

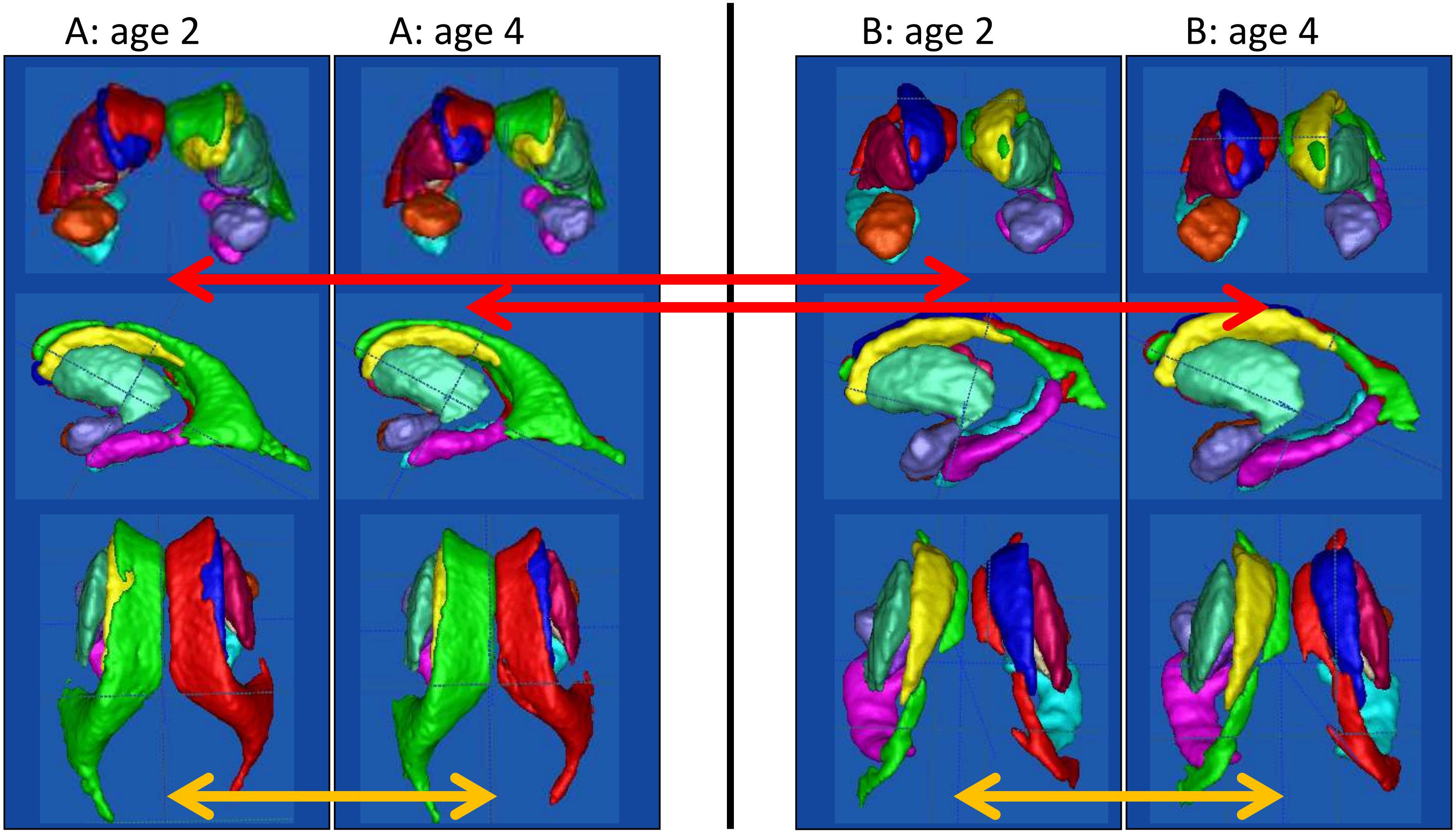

Cross-sectional: Huge changes between sets of shapes

Longitudinal: Subtle changes of sets of shapes with time

Motivation – Study of time dependent data

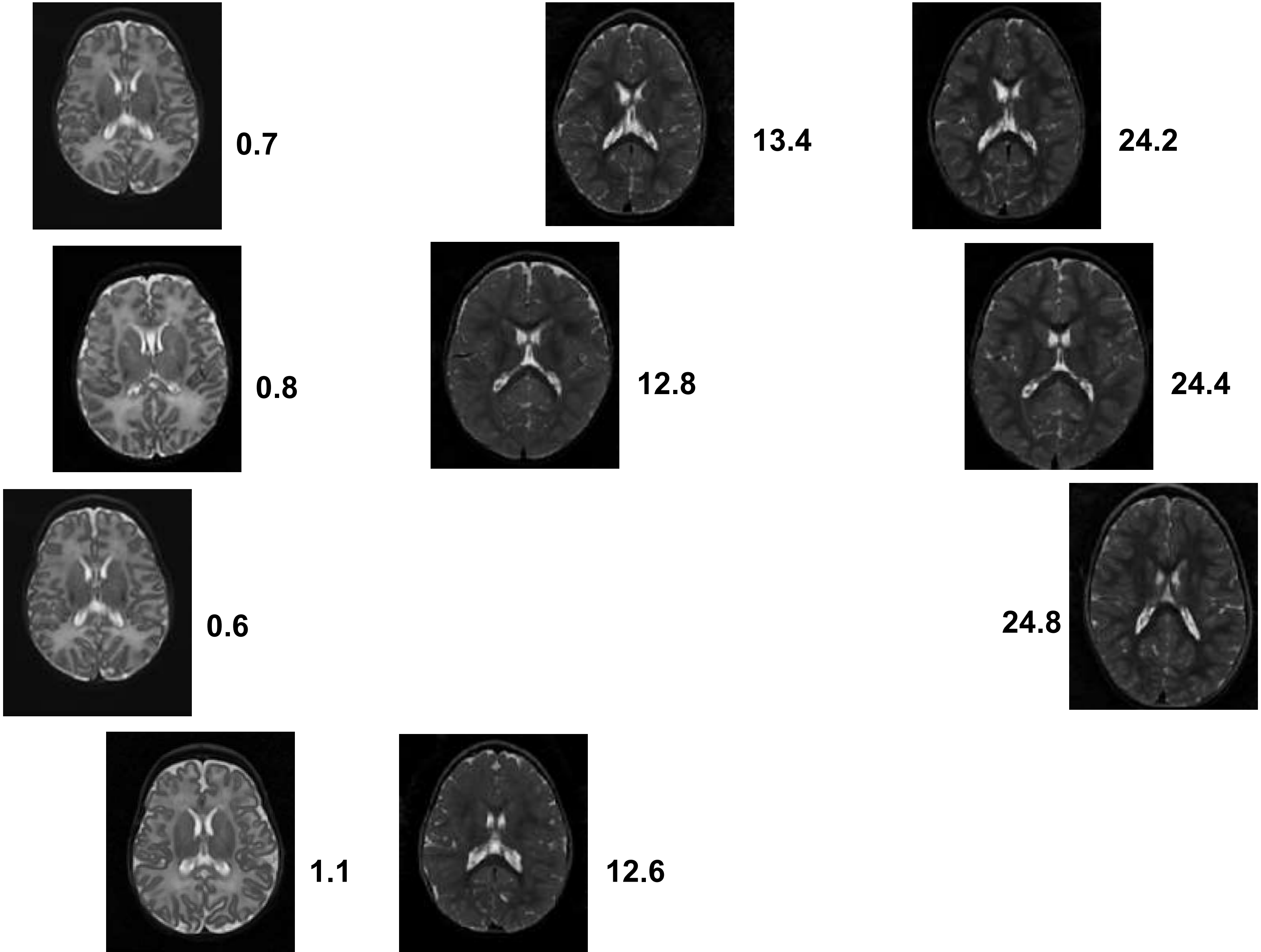

Motivation – Study of longitudinal data

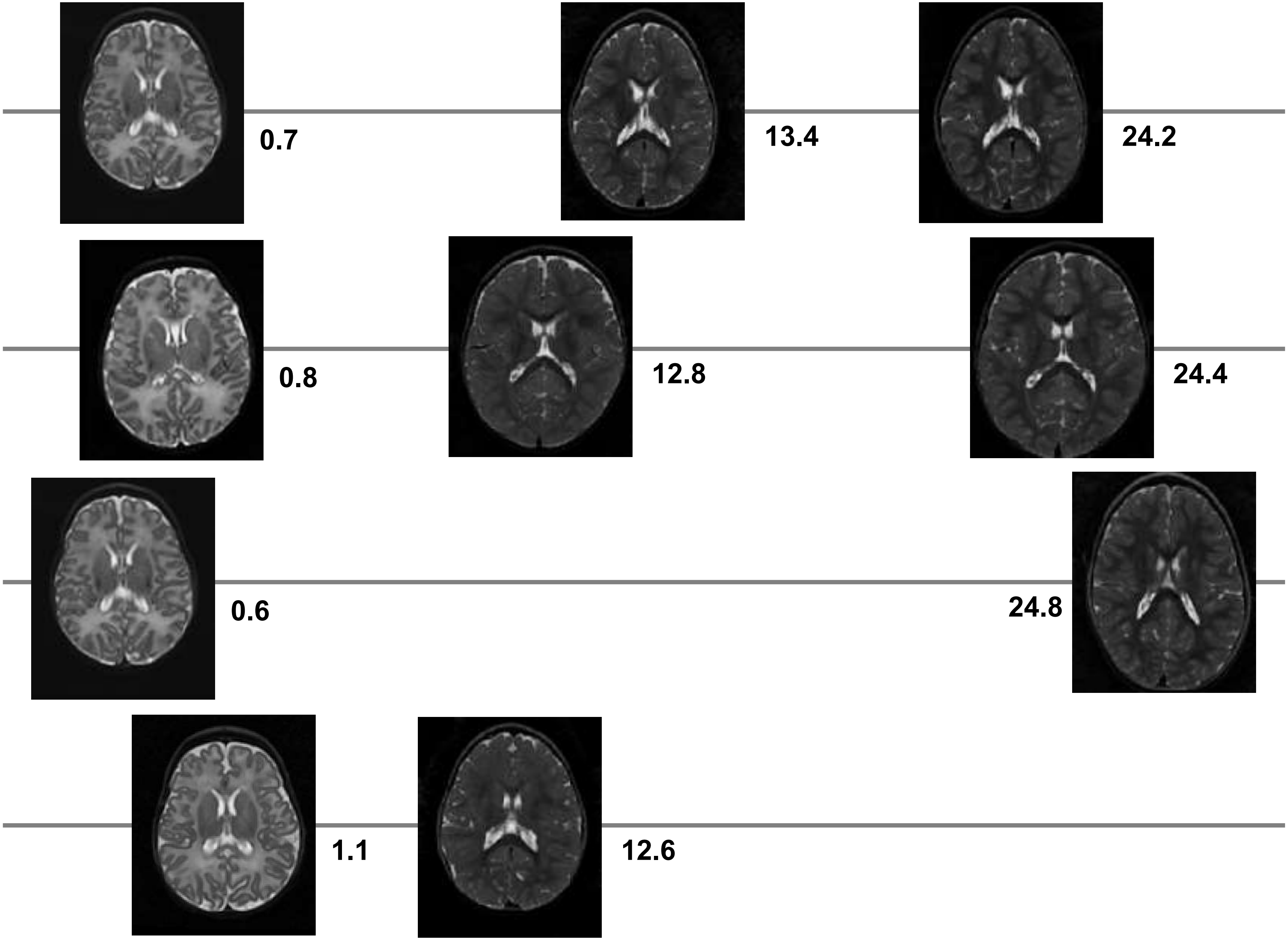

Motivation – Leverage Many Data Formats

Images

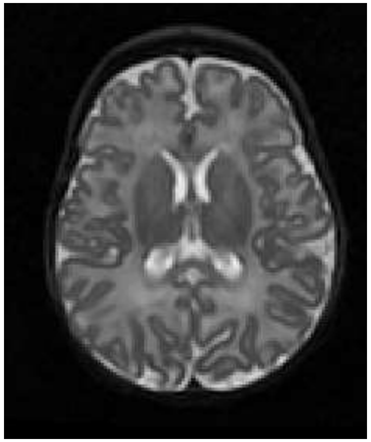

Meshes

Curves

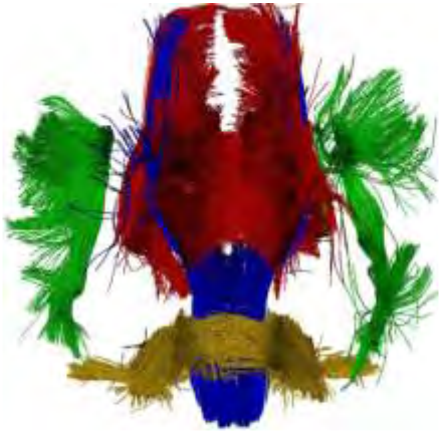

Image: Stanley Durrleman

Point Clouds

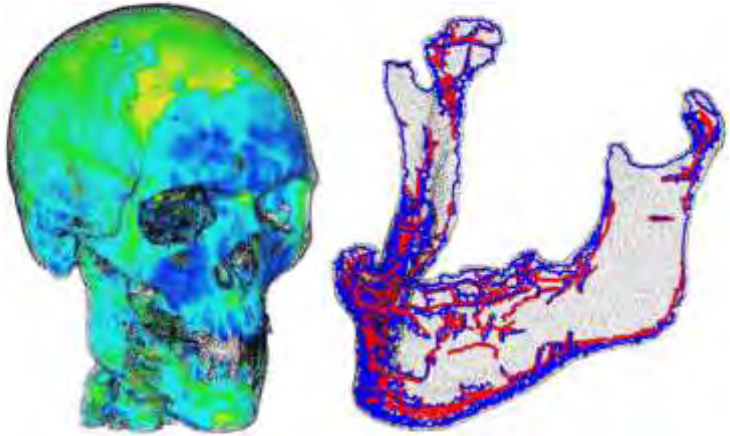

Image: Ming-Ching Chang

Dense Landmarks

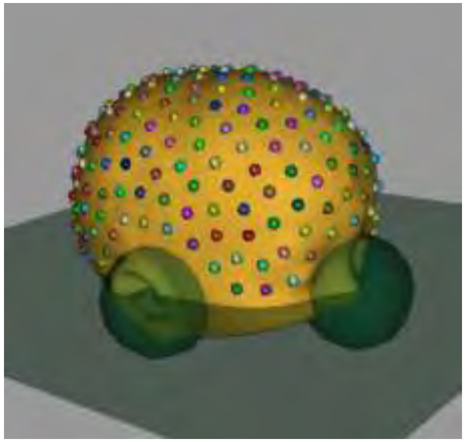

Image: Manasi Datar

Previous Work - Regression

Extension of kernel regression to Riemannian manifolds [**Davis 2007**]

Piecewise geodesic regression for images or shapes [**Khan 2008, Durrleman 2009**]

Geodesic regression for images [**Niethammer 2011, Singh 2013**]

Geodesic regression on Riemannian manifolds [**Fletcher 2011, 2013**]

Shape regression combined with particle correspondence [**Datar 2009**]

Shape splines [**Vialard 2012**]

Previous Work – 4D Statistical Frameworks

Extension of hierarchical linear models to Riemannian manifolds [**Muralidharan 2012**]

Extension of hierarchical linear models for longitudinal images [**Singh 2013**]

Linear mixed effects model for shape with particle correspondence [**Datar 2012**]

Longitudinal atlas construction with time warp [**Durrleman 2009, 2012**]

Longitudinal framework based on stationary velocity fields [**Lorenzi 2011**]

Combining cross-sectional atlas with subject-specific growth [**Hart 2010, Liao 2012**]

Contributions

Goal 1: Develop regression models that capture and describe anatomical change over time

– Suitable for many applications and data formats

Goal 2: Incorporate regression models into a statistical framework for the analysis of longitudinal shape variability

Goal 3: Application and validation of our methods for various clinical application as well as medical imaging tasks, such as segmentation.

Content

- Motivation Longitudinal Modeling
- Acceleration-Controlled Shape Regression
- Geodesic Shape Regression
- Driving Applications:
    - Early Brain Development in Autism
    - Huntington’s Disease (HD)
    - Mandibular Growth
- Concept of Time Warp

4D Shape Modeling from Time-Discrete Data

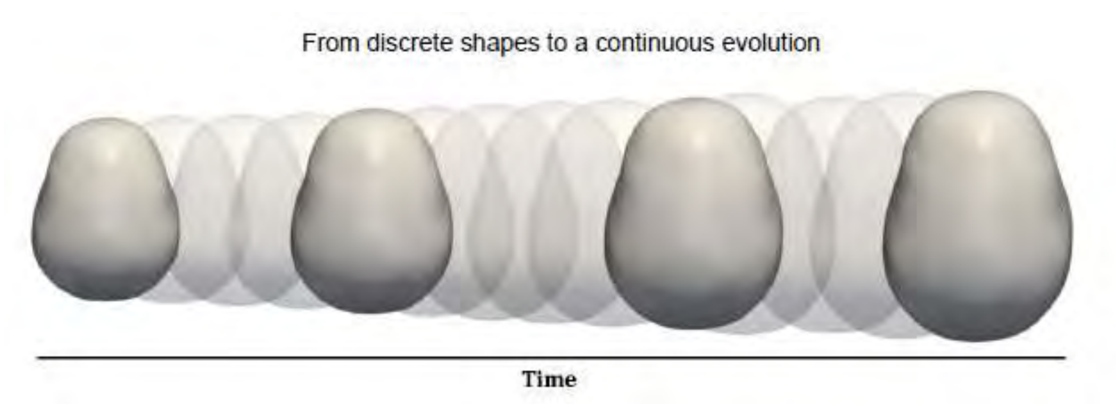

- **Concept**: Given a set of time-discrete shapes, non-uniformly spaced, interpolate a continuous 4D growth model via shape regression.
- **Assumption**: Growth/degeneration of biological tissue is inherently smooth in space and time & nonlinear, locally varying process.
- **Method**: Continuous flow of diffeomorphisms via correspondence-free "currents". *Cost function = Data Matching + Regularity*.

Durrleman, Pennec, Ayache, Trouve, Gerig, MICCAI '09
Fishbaugh, Durrleman, Gerig, MICCAI '11, SPIE'12, MICCAI'12, IPMI'13

Key Observation

Piecewise geodesic regression [Durrleman et. al,. MICCAI 09]

- Shape evolution modeled as the continuous flow of diffeomorphisms
- Geodesics interpolate between observations
- Extension of piecewise linear regression to space of diffeomorphisms

Cannot prevent a loss of regularity at target data

Due to discontinuities in the velocity field

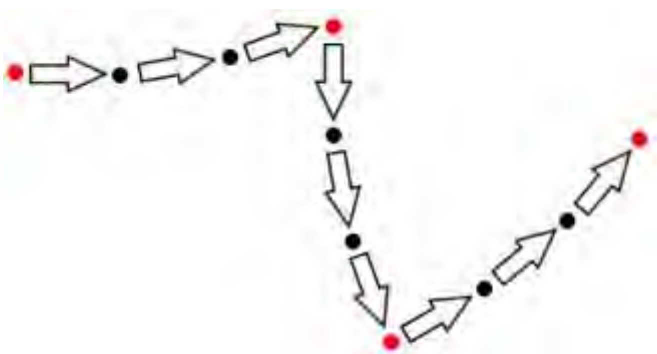

We might desire the velocity field to be differentiable everywhere

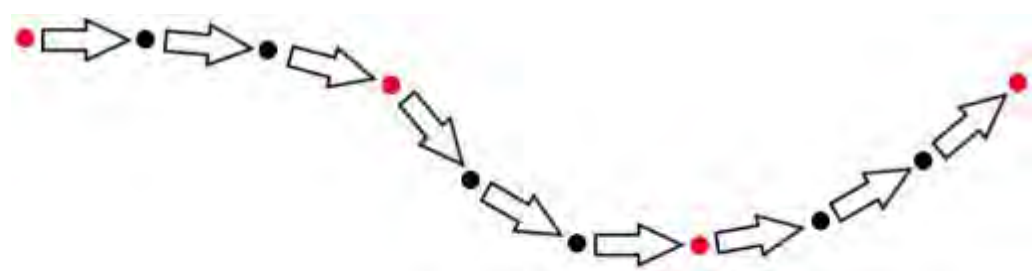

Acceleration Controlled Shape Regression

We define the acceleration field a(x(t)) as a vector field of the form

$$a(x(t)) = \sum_{i=1}^{N} K^V(x(t), x_i(t))\alpha_i(t)$$

x_i: the shape points carrying a point force vector α_i

$K^V(x, y) = exp(-\|x - y\|^2 / \lambda_V^2)$: a Gaussian kernel with standard deviation λ_V

Time varying deformation $\phi_t(x_i)$ given by:

$$\ddot{\phi}_t(x_i) = a(x_i(t))$$

$x_i(0)$: initial position

$\dot{x}_i(0)$: initial velocity

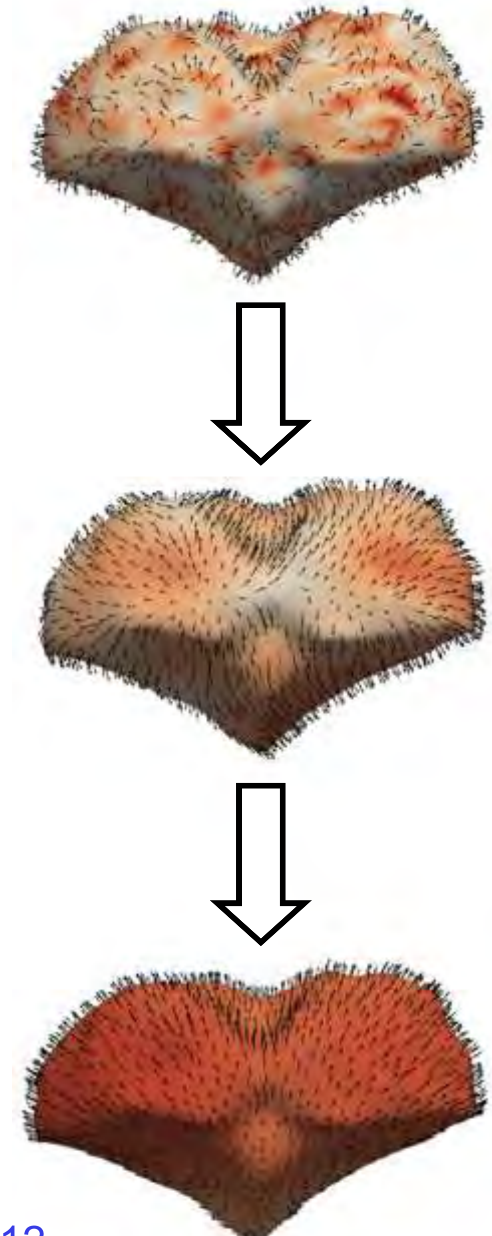

Fishbaugh, MICCAI 2011,12, 13, SPIE 2012

Regression Criterion

Let $\mathbf{x}(t)$, $\mathbf{a}(t)$, and $\boldsymbol{\alpha}(t)$ be the concatenation of the $x_i(t)$'s, $a_i(t)$'s, and the $\alpha_i(t)$'s.

$$E(\dot{\mathbf{x}}(0), \boldsymbol{\alpha}(t)) \;=\; \sum_{t_i} \|\phi_{t_i}(\mathbf{x}(0)) - \mathbf{x}(t_i)\|_{W^*}^2 + \gamma \int_0^T \|\mathbf{a}(t)\|_V^2 \, dt$$

$\|\cdot\|_{W^*}$ is the norm on currents

$\|\mathbf{a}(t)\|_V^2 = \boldsymbol{\alpha}(t) K^V(\mathbf{x}(t), \mathbf{x}(t)) \boldsymbol{\alpha}(t)$

Acceleration Controlled Shape Regression

Evolution of cerebellum from 6 to 24 months

Point forces α

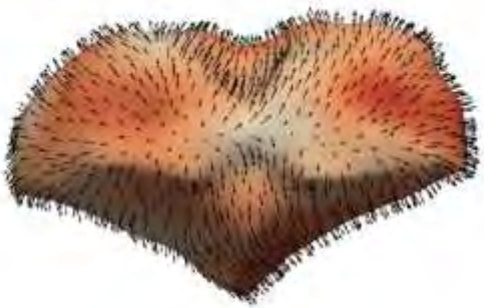

Acceleration

Velocity

Piecewise Geodesic vs Acceleration Controlled

Synthetic experiment comparing piecewise geodesic and acceleration controlled shape regression

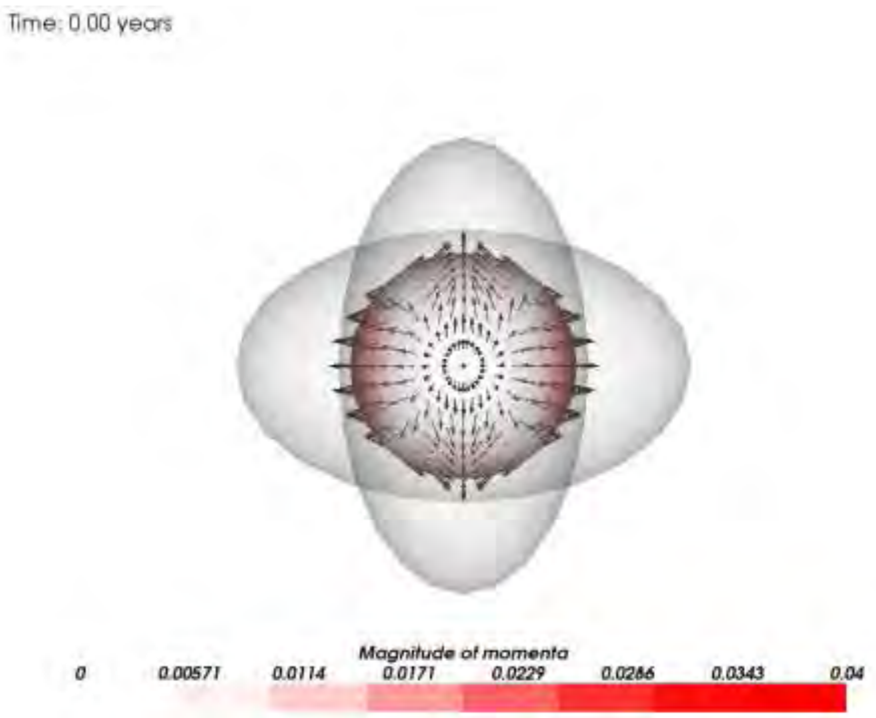

Piecewise geodesic

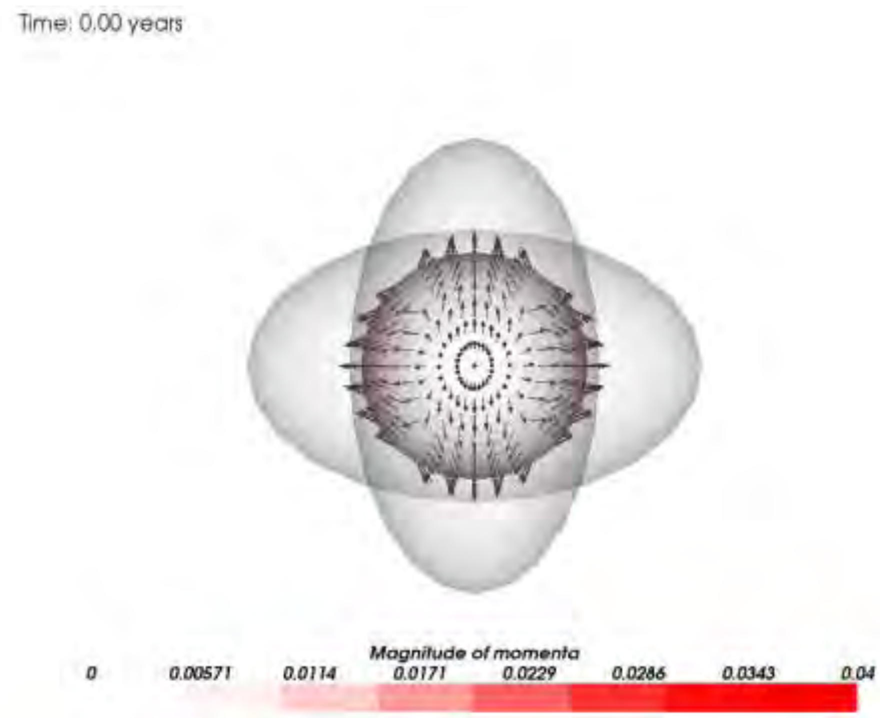

Acceleration controlled

Interpolation Properties

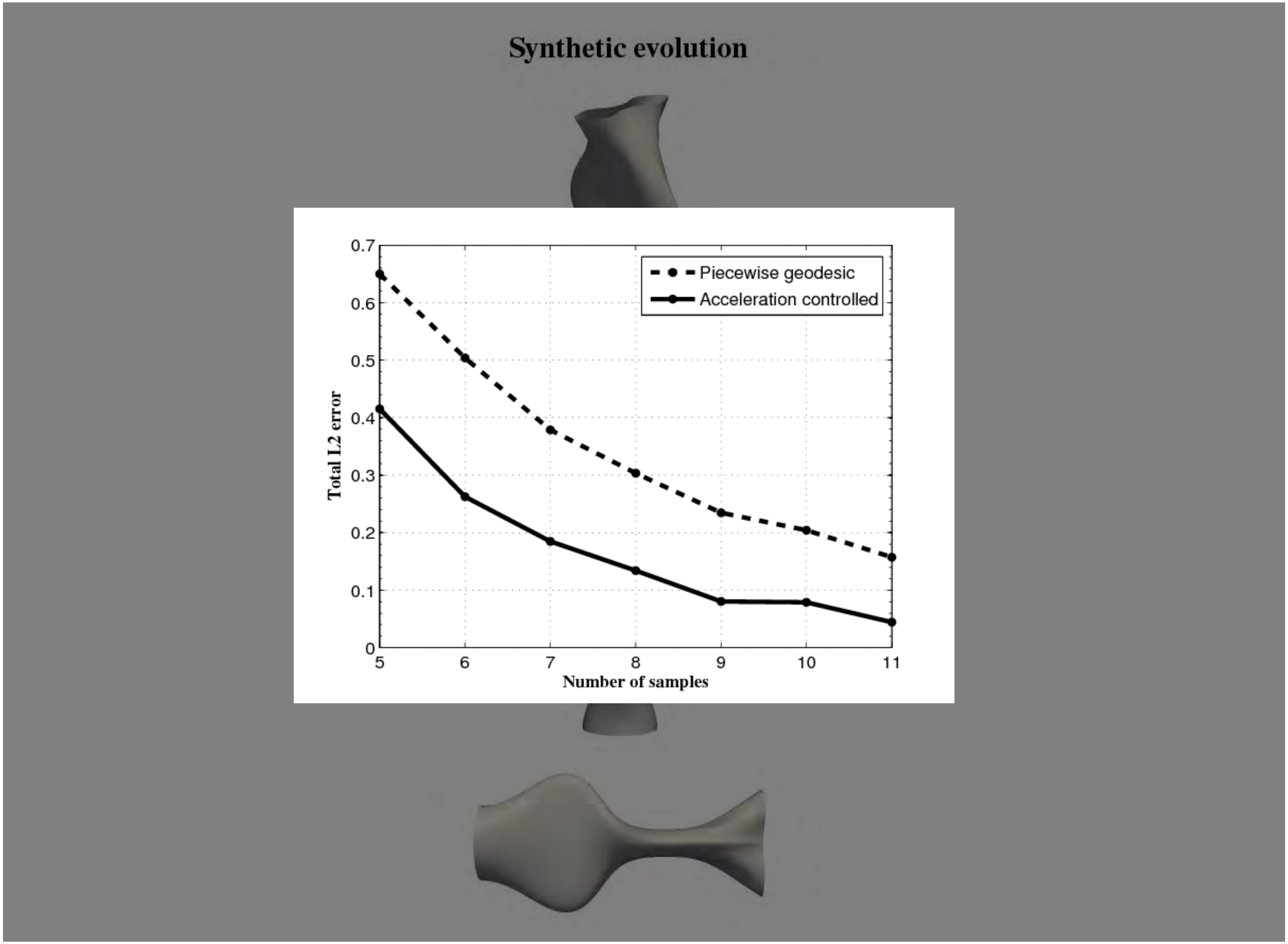

Validation: Infant Brain Growth Data

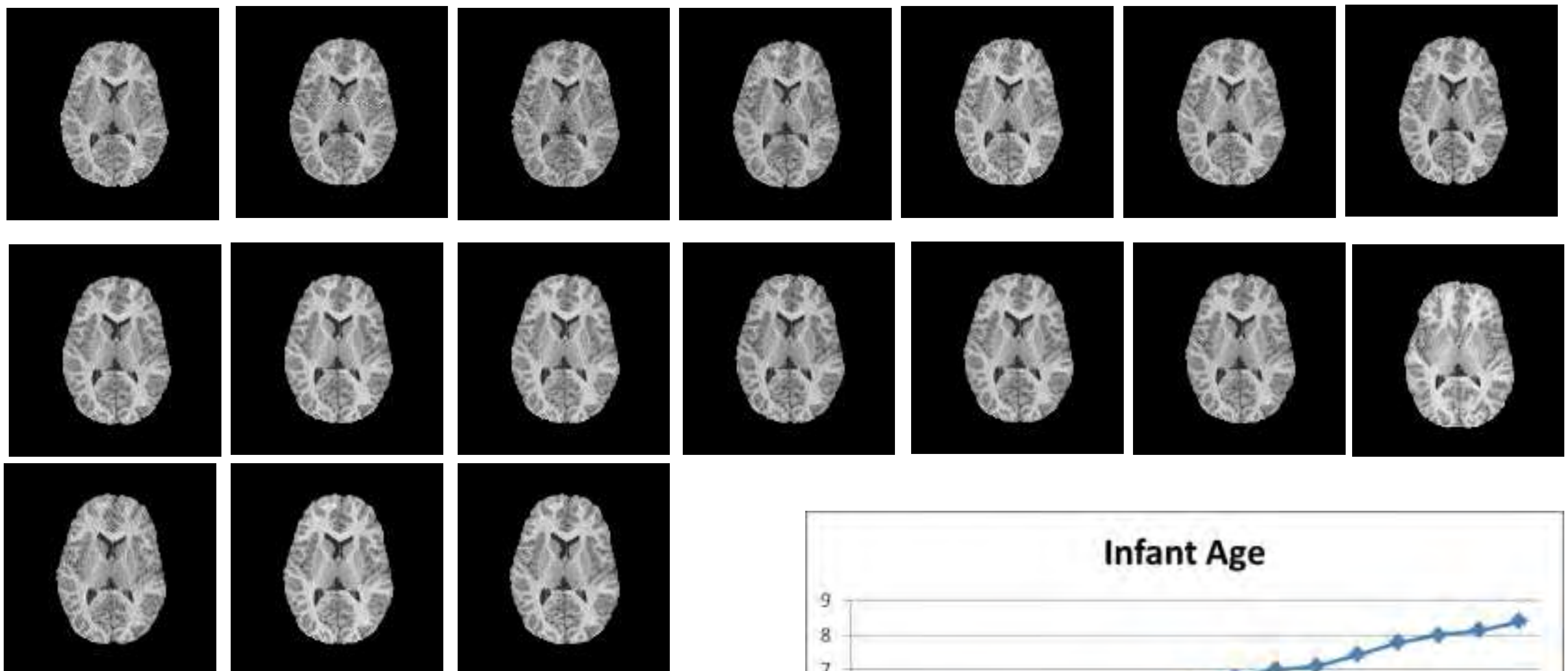

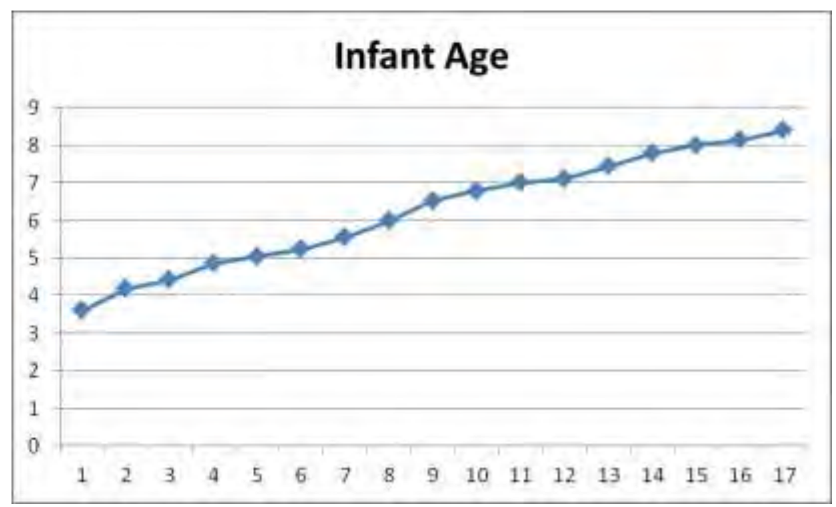

- 17 T1w MRI
- Age range 3.6 – 8.4yrs
- Courtesy Jay Giedd, NIMH

Validation

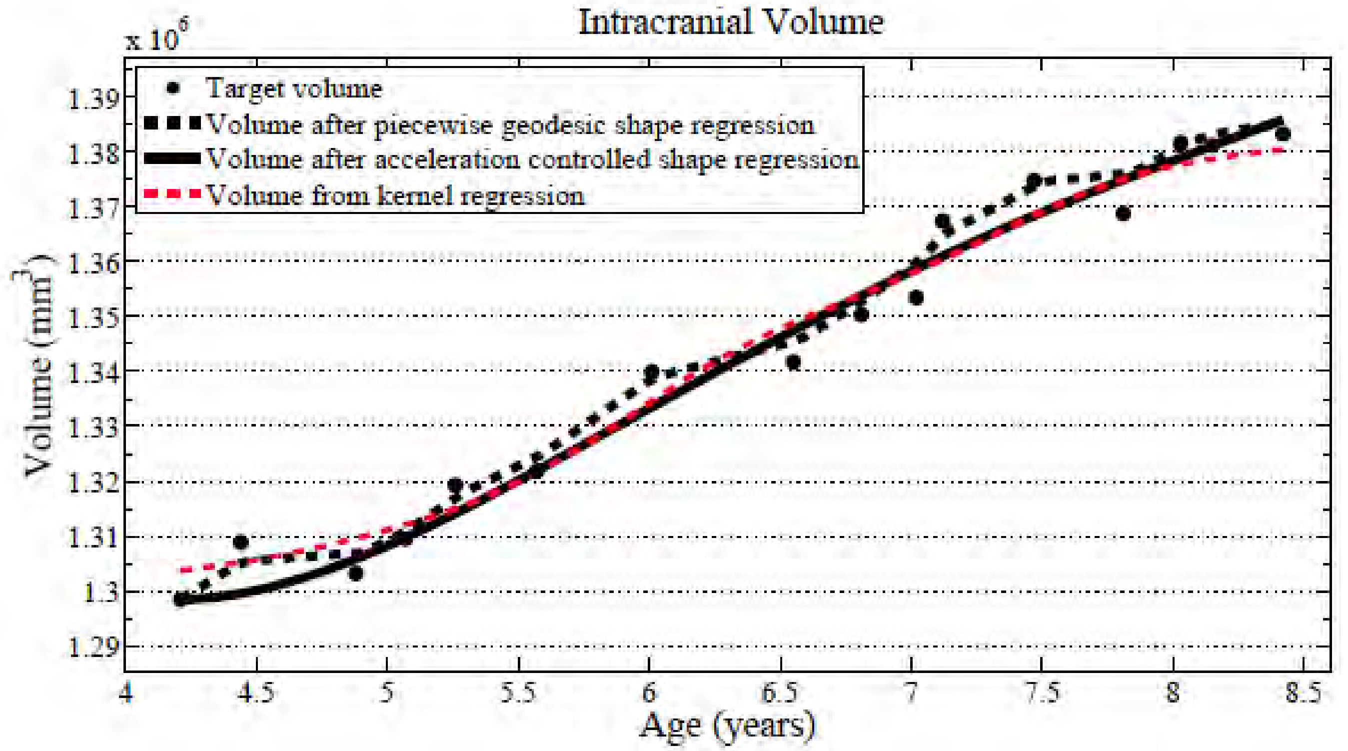

Volume measurements derived from our growth model are consistent with a kernel regression (σ = 0.5) performed on the sparse volume measurements. Our model describes the continuous evolution of shape and volume is measured after regression.

Fishbaugh et al., MICCAI 2011

Validation ctd.

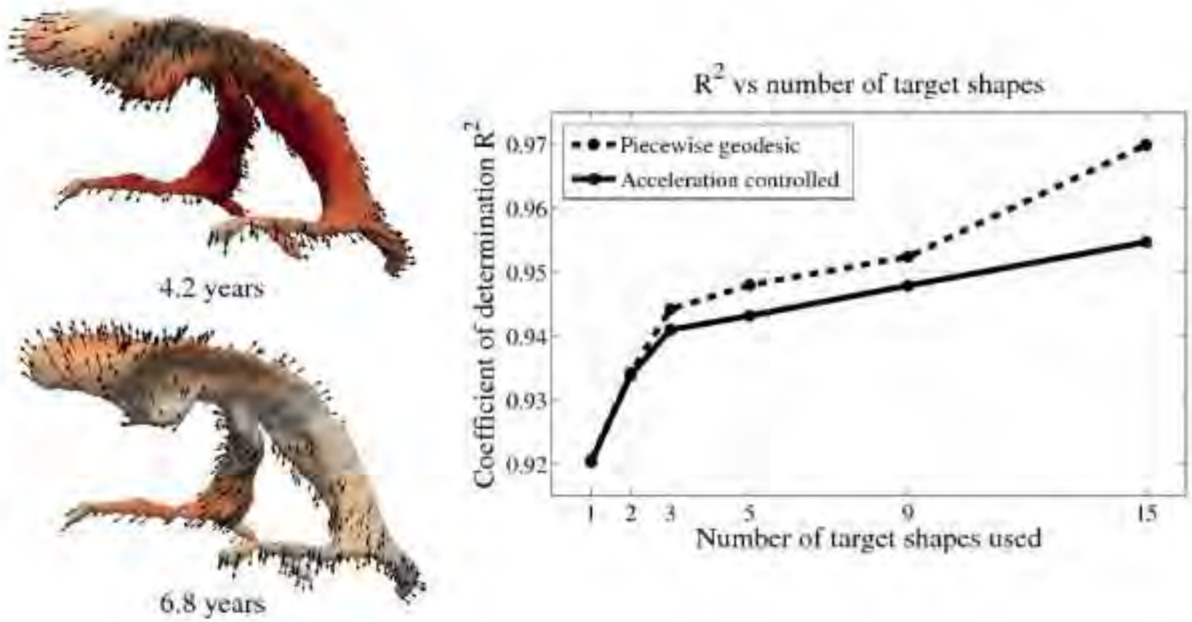

Fig. 3. Left: Snapshots from a continuous shape evolution of lateral ventricles estimated by our regression model. Acceleration vectors are displayed on the surface, with color denoting magnitude. **Right:** The impact of the number of target shapes on R^2.

Fishbaugh et al., MICCAI 2011

Determination R^2

Definitions [edit]

A data set has values y_i, each of which has an associated modelled value f_i (also sometimes referred to as $\hat{y}_i$). Here, the values y_i are called the observed values and the modelled values f_i are sometimes called the predicted values.

In what follows $\bar{y}$ is the mean of the observed data:

$$\bar{y} = \frac{1}{n}\sum_{i=1}^{n} y_i$$

where n is the number of observations.

The "variability" of the data set is measured through different sums of squares:[disambiguation needed]

$SS_\text{tot} = \sum_i (y_i - \bar{y})^2$, the total sum of squares (proportional to the sample variance);

$SS_\text{reg} = \sum_i (f_i - \bar{y})^2$, the regression sum of squares, also called the explained sum of squares.

$SS_\text{res} = \sum_i (y_i - f_i)^2$, the sum of squares of residuals, also called the residual sum of squares.

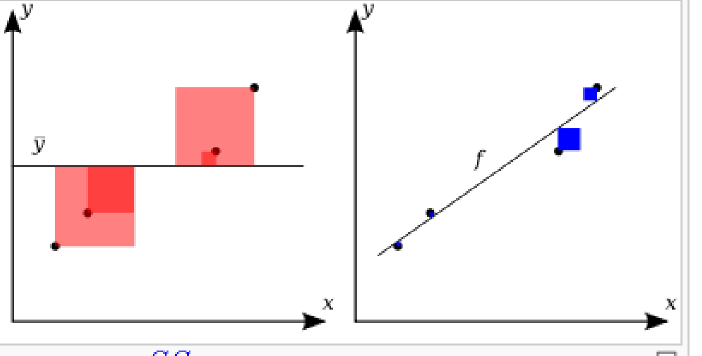

$$R^2 = 1 - \frac{SS_\text{res}}{SS_\text{tot}}$$

The better the linear regression (on the right) fits the data in comparison to the simple average (on the left graph), the closer the value of R^2 is to one. The areas of the blue squares represent the squared residuals with respect to the linear regression. The areas of the red squares represent the squared residuals with respect to the average value.

The notations SS_R and SS_E should be avoided, since in some texts their meaning is reversed to **R**esidual sum of squares and **E**xplained sum of squares, respectively.

The most general definition of the coefficient of determination is

$$R^2 \equiv 1 - \frac{SS_\text{res}}{SS_\text{tot}}.$$

Determination R^2

In statistics, the **coefficient of determination**, denoted R^2 or r^2 and pronounced **R squared**, indicates how well data fit a statistical model – sometimes simply a line or curve. It is a statistic used in the context of statistical models whose main purpose is either the prediction of future outcomes or the testing of hypotheses, on the basis of other related information. It provides a measure of how well observed outcomes are replicated by the model, as the proportion of total variation of outcomes explained by the model.[1]

There are several definitions of R^2 that are only sometimes equivalent. One class of such cases includes that of simple linear regression where r^2 is used instead of R^2. In this case, if an intercept is included, then r^2 is simply the square of the sample correlation coefficient (i.e., r) between the outcomes and their predicted values. If additional explanators are included, R^2 is the square of the coefficient of multiple correlation. In both such cases, the coefficient of determination ranges from 0 to 1.

Important cases where the computational definition of R^2 can yield negative values, depending on the definition used, arise where the predictions that are being compared to the corresponding outcomes have not been derived from a model-fitting procedure using those data, and where linear regression is conducted without including an intercept. Additionally, negative values of R^2 may occur when fitting non-linear functions to data.[2] In cases where negative values arise, the mean of the data provides a better fit to the outcomes than do the fitted function values, according to this particular criterion.[3]

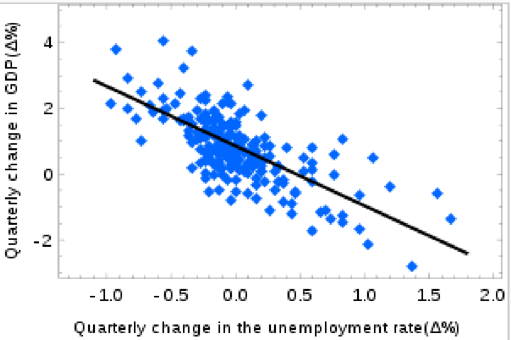

Ordinary least squares regression of Okun's law. Since the regression line does not miss any of the points by very much, the R^2 of the regression is relatively high.

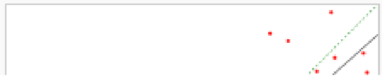

Interpolation Properties

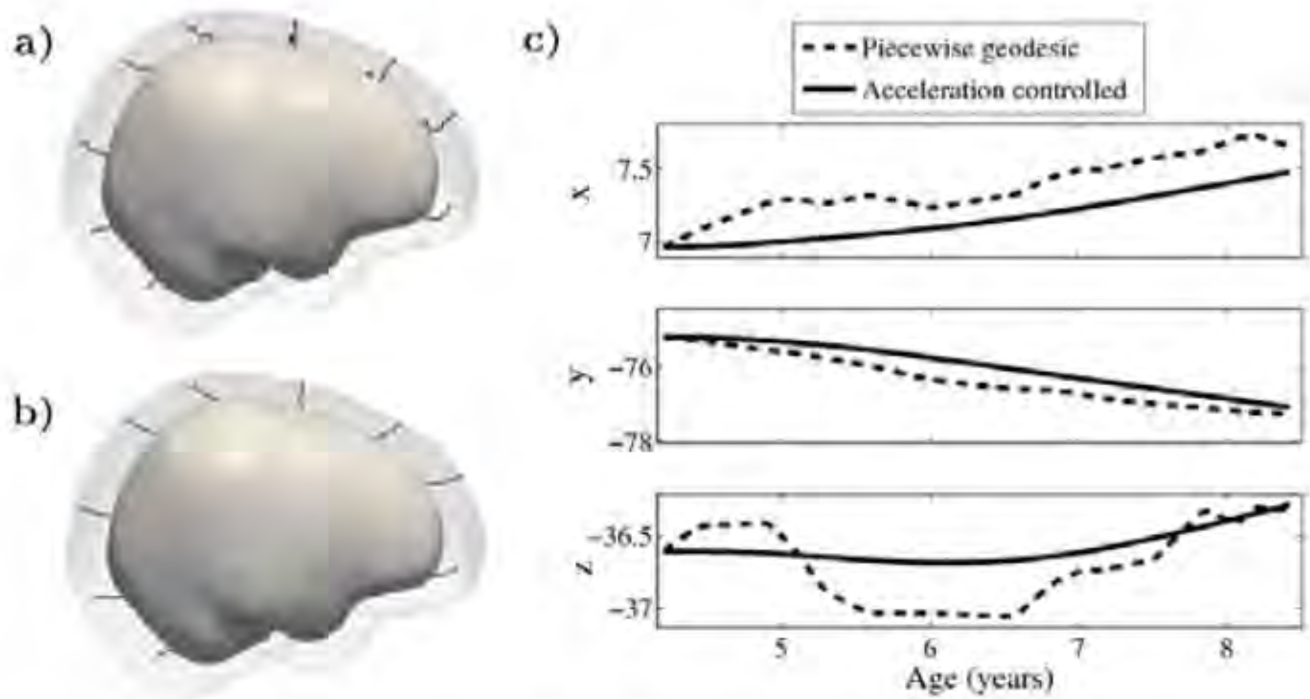

Fig. 1. **a)** and **b)** Shape evolution from baseline (solid) to final configuration (transparent) using a model based on piecewise geodesics (a) and our method (b) with point trajectories for selected particles displayed as black lines. **c)** The path of a point on the forebrain is decomposed into coordinates. Growth is estimated using 15 target shapes, highlighting the speed discontinuities present in the piecewise geodesic evolution.

Fishbaugh et al., MICCAI 2011

Summary Acceleration-controlled Shape Regression

Benefits:

- More biologically realistic trajectories
- Nice interpolation properties

Drawbacks:

- Not compact or generative
- 4D shape statistics to be developed

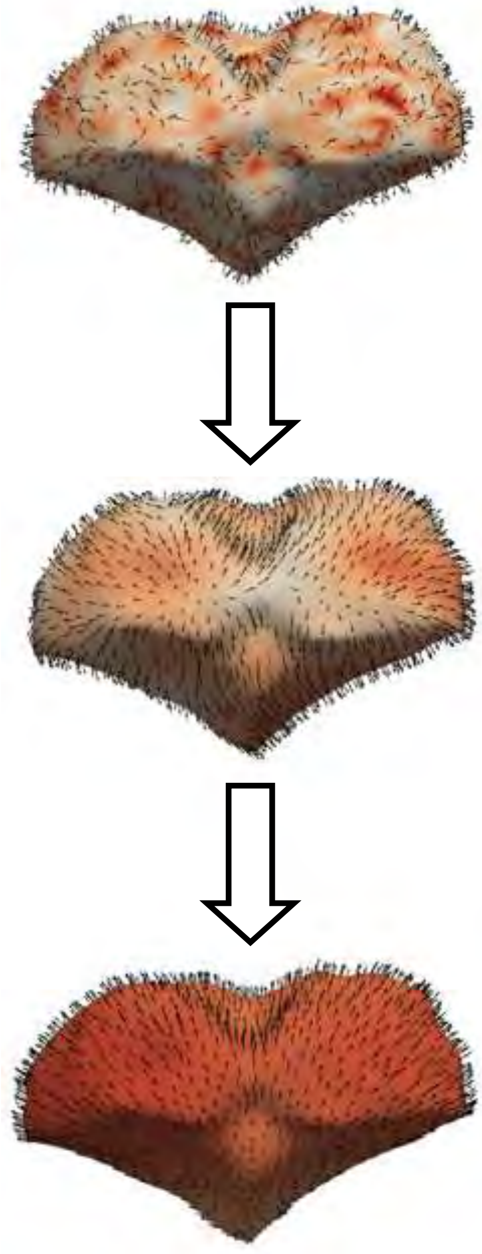

Content

- Motivation Longitudinal Modeling
- Acceleration-Controlled Shape Regression
- Geodesic Shape Regression
- Driving Applications:
  - Early Brain Development in Autism
  - Huntington's Disease (HD)
  - Mandibular Growth
- Concept of Time Warp

Geodesic Shape Regression

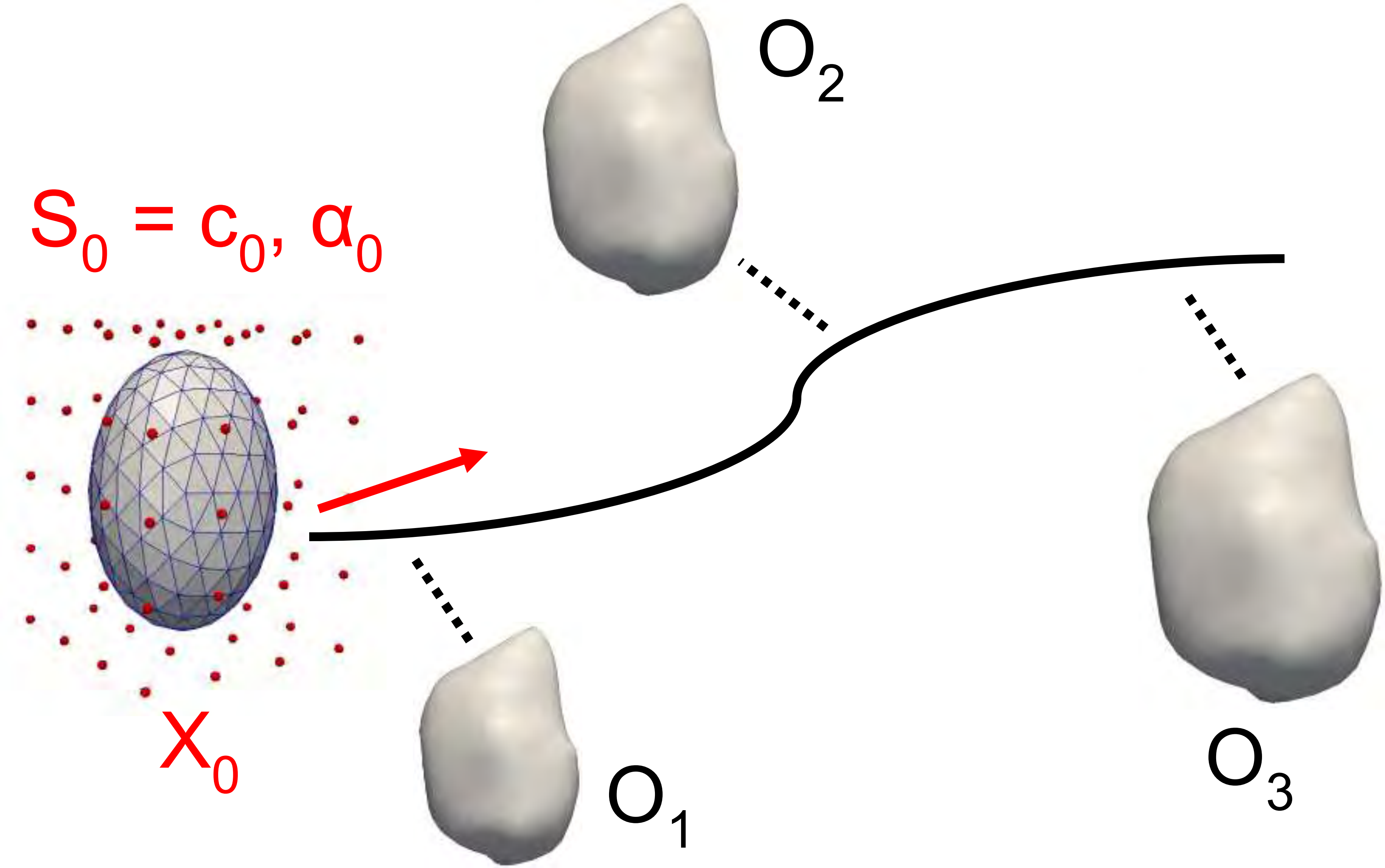

Control Point Formulation

$S_0 = c_0, \alpha_0$

Geodesic shooting to evolve control points

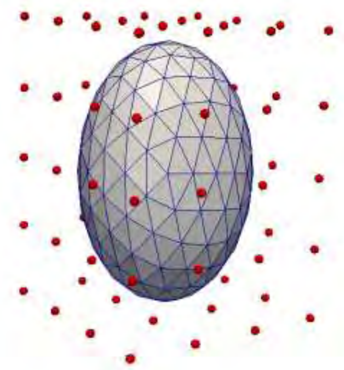

$$\begin{cases} \dot{c}_i(t) = \sum_{p=1}^{N_c} K(c_i(t), c_p(t))\alpha_p(t) \\ \dot{\alpha}_i(t) = -\sum_{p=1}^{N_c} \alpha_i(t)^t \alpha_p(t) \nabla_1 K(c_i(t), c_p(t)) \end{cases}$$

Trajectory of control points defines **flow** of diffeomorphisms

$$\dot{\phi}_t(x) = v(x,t) = \sum_{p=1}^{N_c} K(x, c_p(t))\alpha_p(t)$$

Regression Criterion

$S_0 = c_0, \alpha_0$

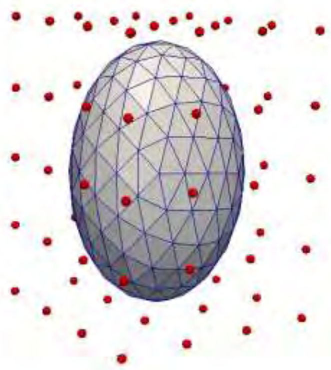

$$E(\mathbf{X}_0, \mathbf{S}_0) = \sum_{i=1}^{N_{obs}} \frac{1}{2\lambda^2} D(\mathbf{X}(t_i), \mathbf{O}_{t_i}) + L(\mathbf{S}_0)$$

D is squared distance on currents

$$D(\mathbf{X}(t_i), \mathbf{O}_{t_i}) = ||(\phi_{t_i}(\mathbf{X}_0) - \mathbf{O}_{t_i})||^2_{W^*}$$

Regularity defined by kinetic energy of control points

$$L(\mathbf{S}_0) = \sum_{p,q} \alpha_{0,p}^t K(c_{0,p}, c_{0,q}) \alpha_{0,q}$$

Geodesic Shape Regression Experiments

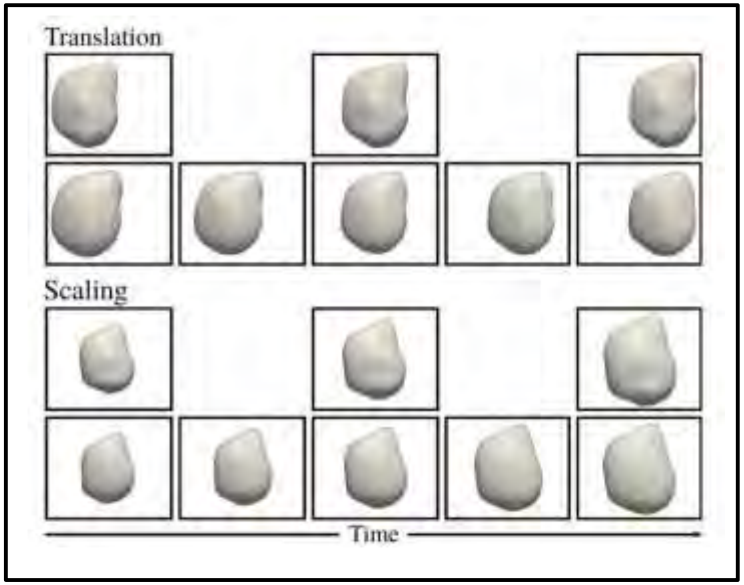

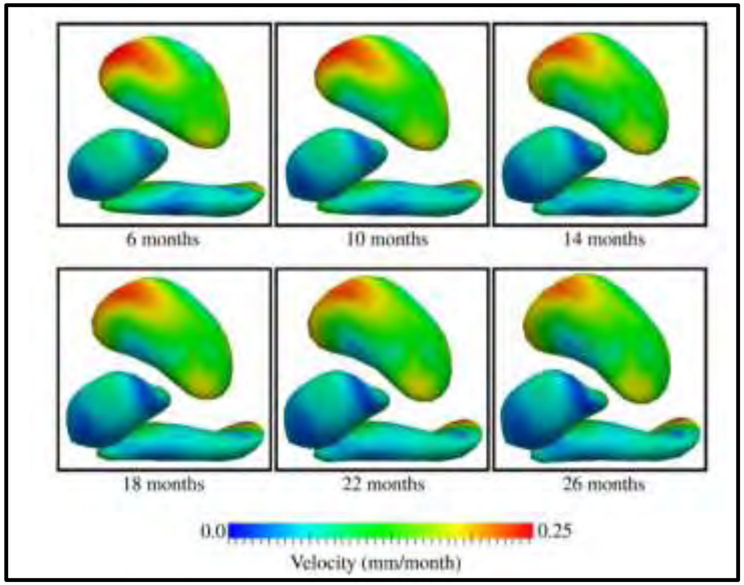

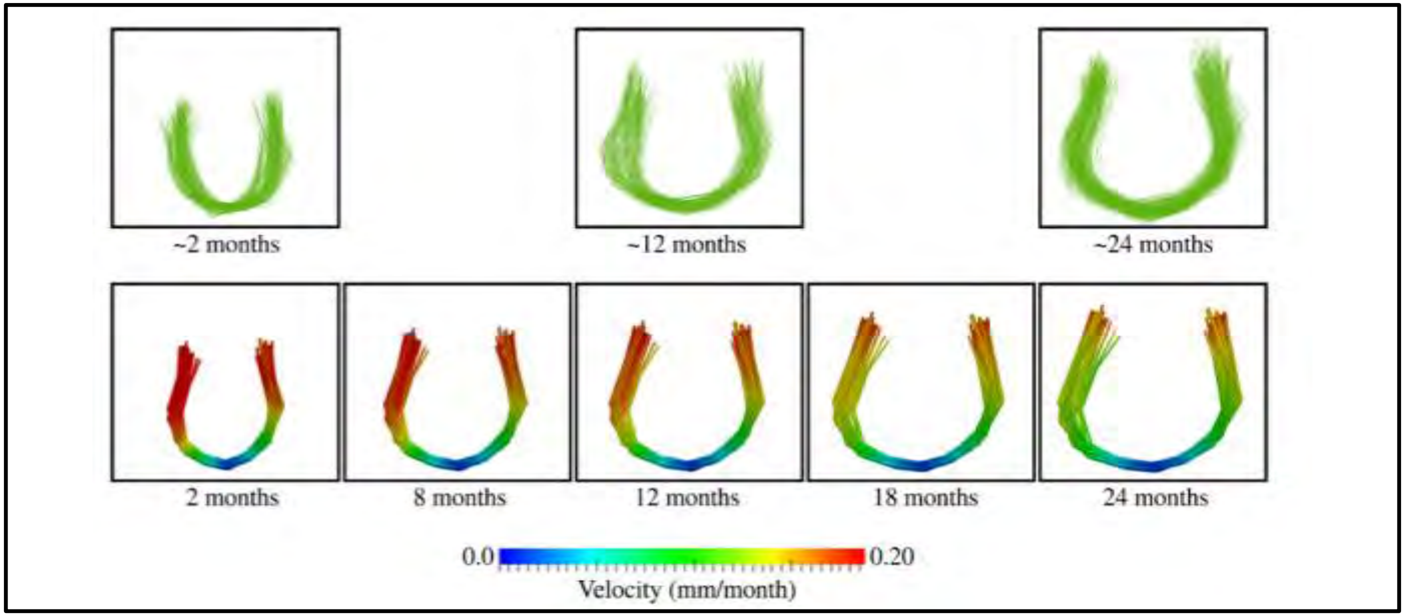

Geodesic Image Regression

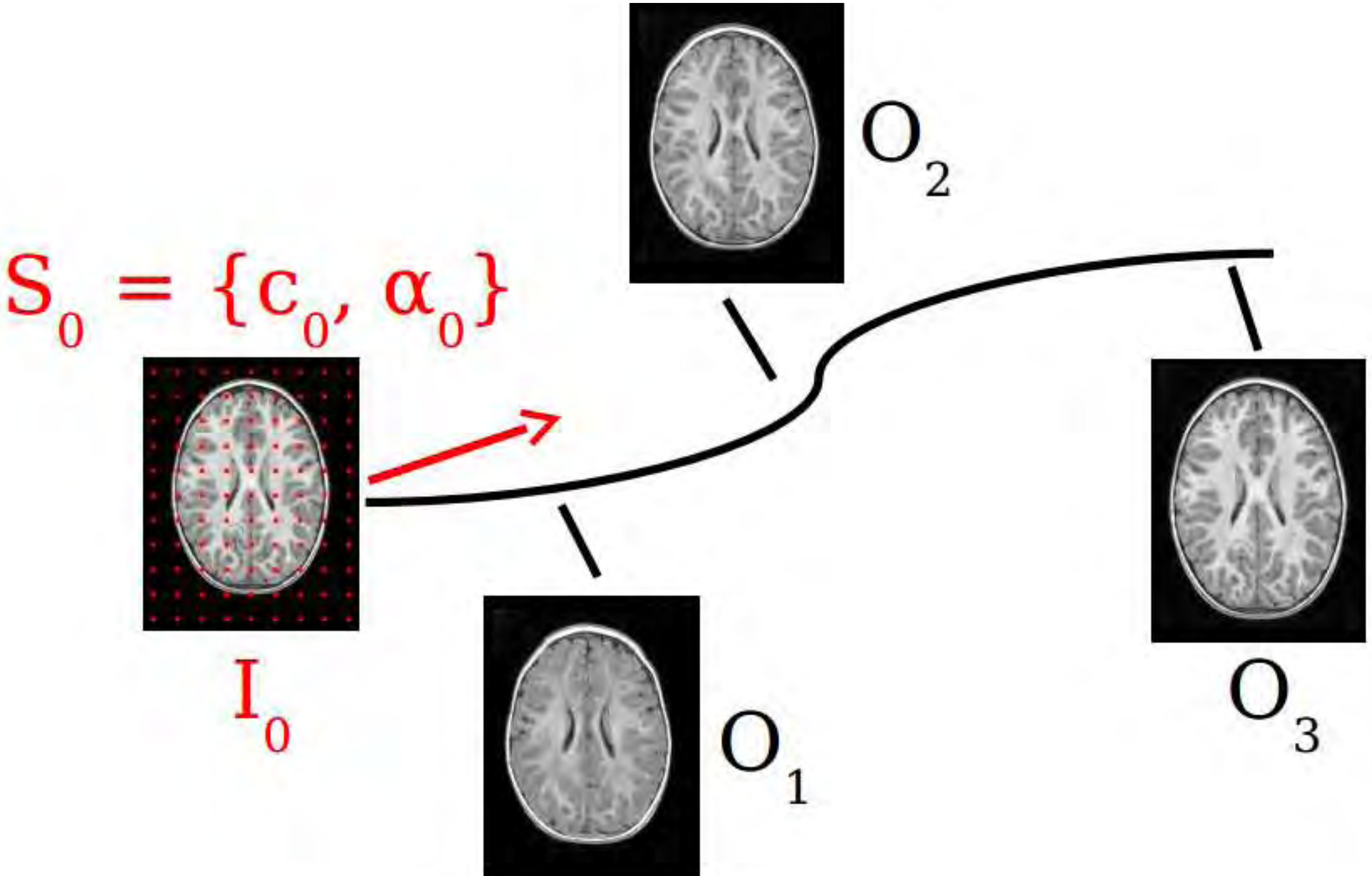

Method

Initial state $S_0 = \{c_0, \alpha_0\}$ parameterize **geodesic** flow

$$\begin{cases} \dot{c}_i(t) = \sum_{p=1}^{N_c} K(c_i(t), c_p(t))\alpha_p(t) \\ \dot{\alpha}_i(t) = -\sum_{p=1}^{N_c} \alpha_i(t)^t \alpha_p(t) \nabla_1 K(c_i(t), c_p(t)) \end{cases}$$

Deformation applied to pixel locations **y** by solving

$$\dot{\mathbf{Y}}(t, \mathbf{y}) = -[d_{\mathbf{y}} \mathbf{Y}(t, \mathbf{y})] v(\mathbf{y}, t)$$

Deformed images constructed by interpolation

$$I(t) = \mathbf{I}_0(\mathbf{Y}(t))$$

Summary of Method

1) **Shoot** control points

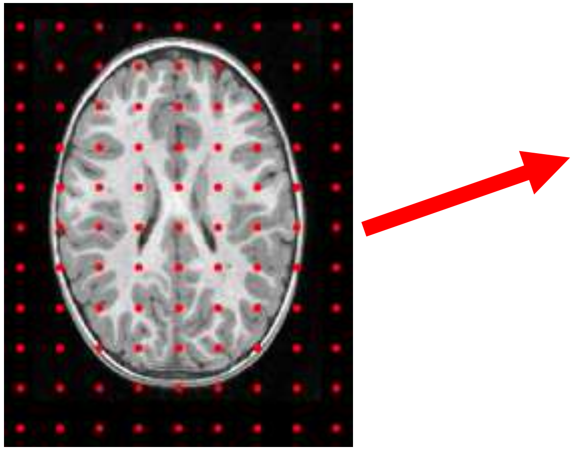

2) **Trajectory** defines flow

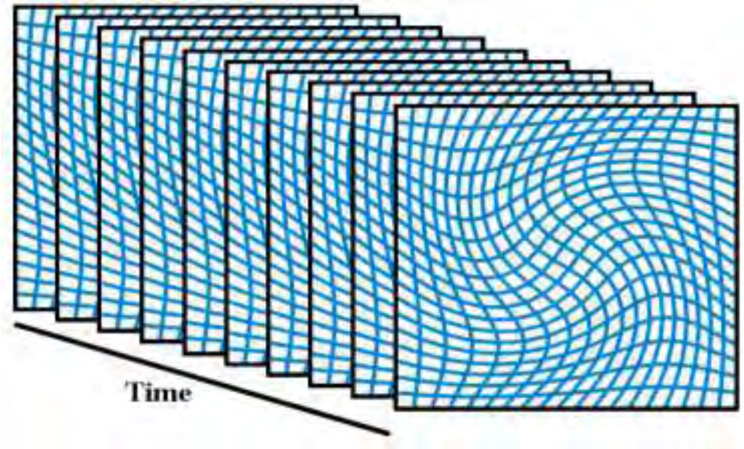

3) **Flow** pixel locations

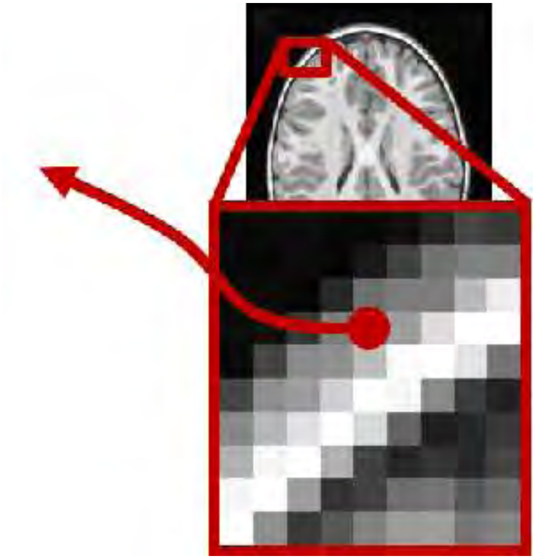

4) **Interpolate** in baseline image

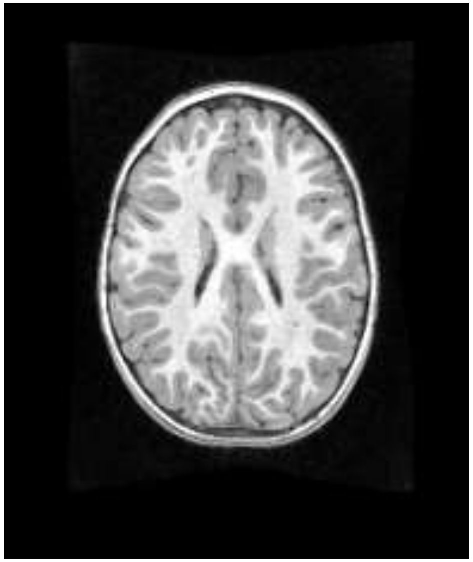

Regression Criterion

$$E(\mathbf{I}_0, \mathbf{S}_0) = \sum_{i=1}^{N_{obs}} \frac{1}{2\lambda^2} D(\mathbf{Y}(t_i)) + \operatorname{Reg}(\mathbf{S}_0) + \gamma_{\text{sp}} \sum_{i=1}^{N_c} ||\alpha_i(t_0)||$$

$$\operatorname{Reg}(\mathbf{S}_0) = \sum_{p,q} \alpha_{0,p}^t K(c_{0,p}, c_{0,q}) \alpha_{0,q}$$

Subject to

$$\begin{array}{ll} \textbf{Shoot} & \left\{ \begin{array}{ll} \dot{\mathbf{S}}(t) = F(\mathbf{S}(t)) & \text{with } \mathbf{S}(0) = \{\mathbf{c}_0, \boldsymbol{\alpha}_0\} \\ \dot{\mathbf{Y}}(t) = G(\mathbf{Y}(t), \mathbf{S}(t)) & \text{with } \mathbf{Y}(0, \mathbf{y}) = \mathbf{y} \end{array} \right. \\ \textbf{Flow} & \end{array}$$

Solved via **Fast Iterative Shrinkage Thresholding Algorithm**

- Use previous gradient of criterion **without** L1 penalty
- **Threshold** momentum vectors with small magnitude

Brain Atrophy in Alzheimer's Disease (3D)

T1W images of **same** patient over time (~2,000,000 voxels)

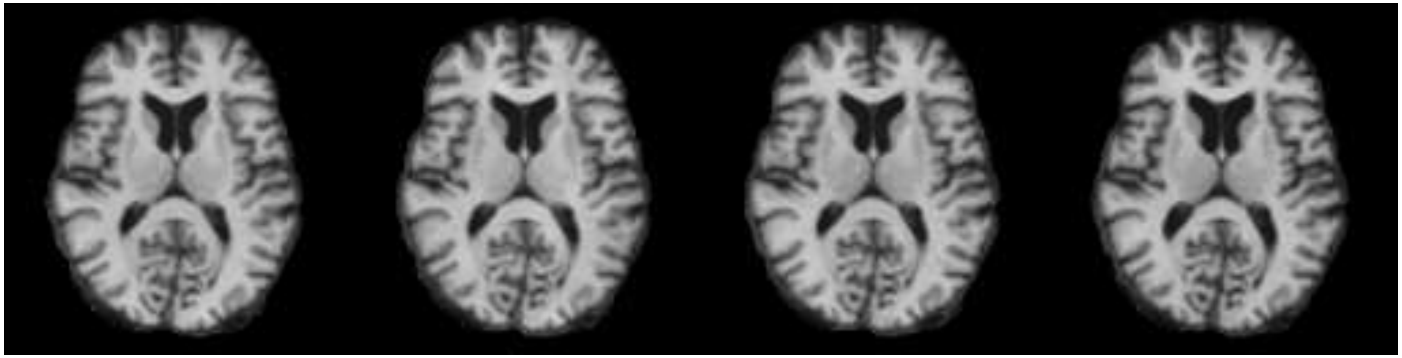

70.75 years **71.38 years** **71.78 years** **72.79 years**

Six years **predicted** brain atrophy

35,937

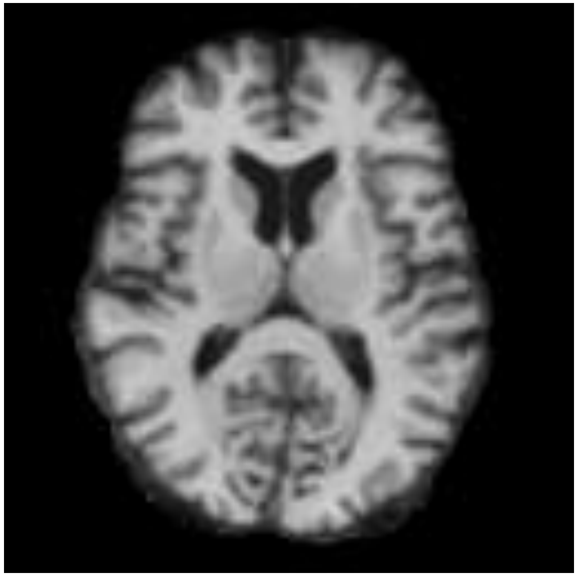

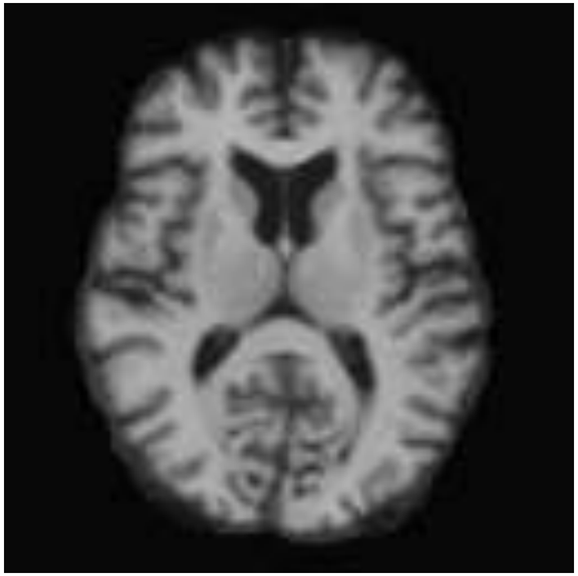

215

Geodesic Regression of Images + Shapes

$$E(\mathbf{S}_0, I_0, X_0) = \sum_{t_i} \left(\lambda_{S_{t_i}} d_S(X(t_i), X_i) + \lambda_{I_{t_i}} d_I(I(t_i), I_i)\right) + \mathrm{Reg}(\mathbf{S}_0)$$

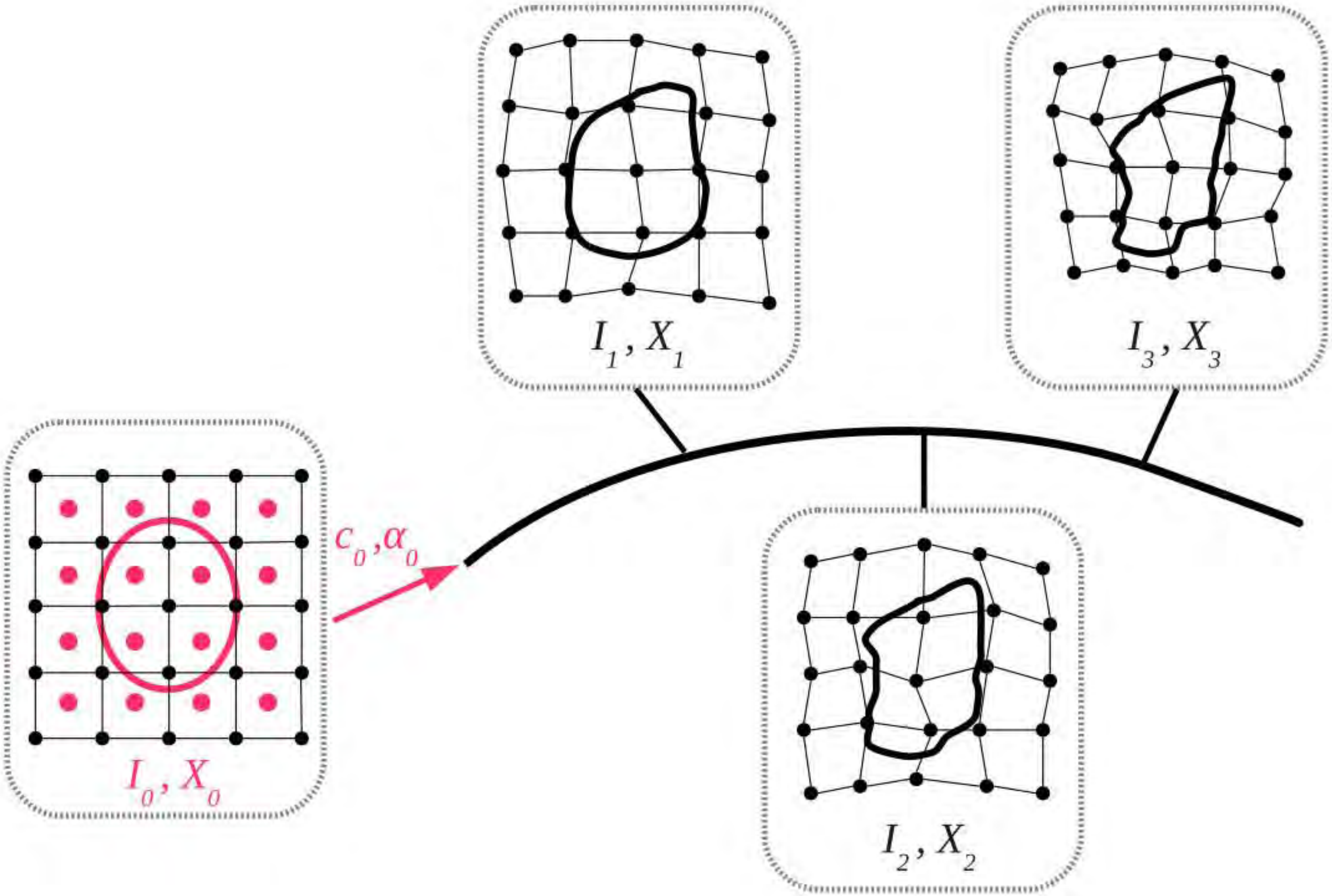

Summary of Regression Models

Complimentary regression models:

Acceleration controlled

- Generic and flexible
- Nice interpolation properties
- Using currents → Independent on parametrization

Geodesic

- Compact statistical model
- Extrapolation
- Limited to specific growth types

Applicable to a wide variety of data formats (2D or 3D) in any combination

- Images
- Meshes
- Curves
- Point clouds or landmark points

Content

- Motivation Longitudinal Modeling
- Acceleration-Controlled Shape Regression
- Geodesic Shape Regression
- Driving Applications:
  - Early Brain Development in Autism
  - Huntington's Disease (HD)
  - Mandibular Growth
- Concept of Time Warp

Driving Motivation: Autism

Complex neurodevelopmental disorder.

Many subjects require long-term care and costly therapy.

Reports of autism cases per 1,000 children grew dramatically in the U.S. from 1996 to 2007.

Prevention?

Treatment?

The earlier intervention starts, the better the outcome

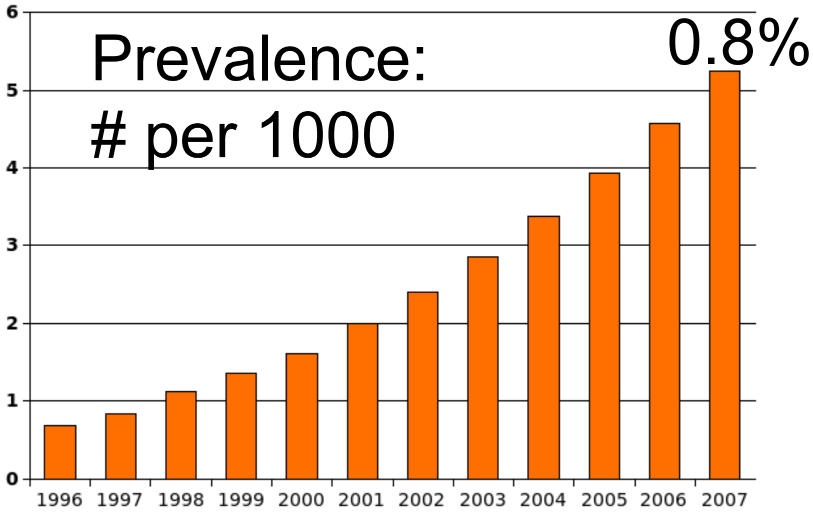

ACE-IBIS Research: Neuroimaging of early brain development:

- Mechanisms of cause and brain alterations
- Towards better & earlier therapy

Autism Centers: Therapy

Autism: Longitudinal Infant Neuroimaging Study

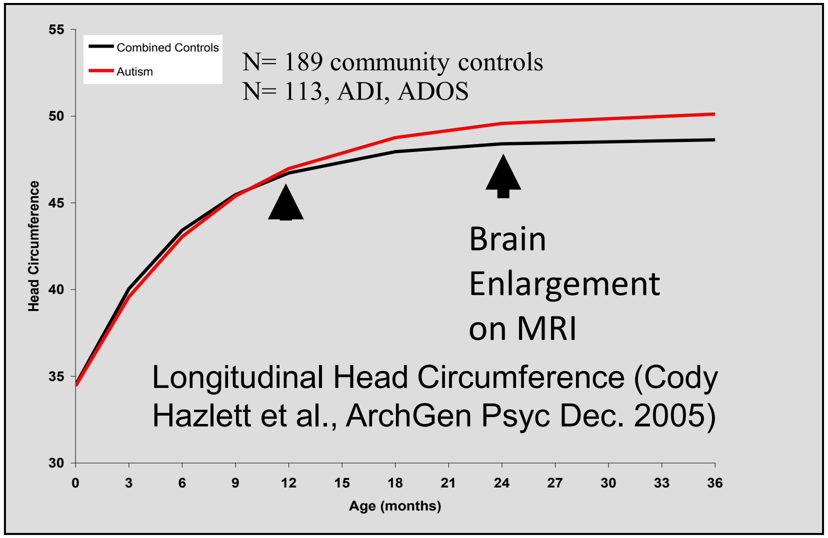

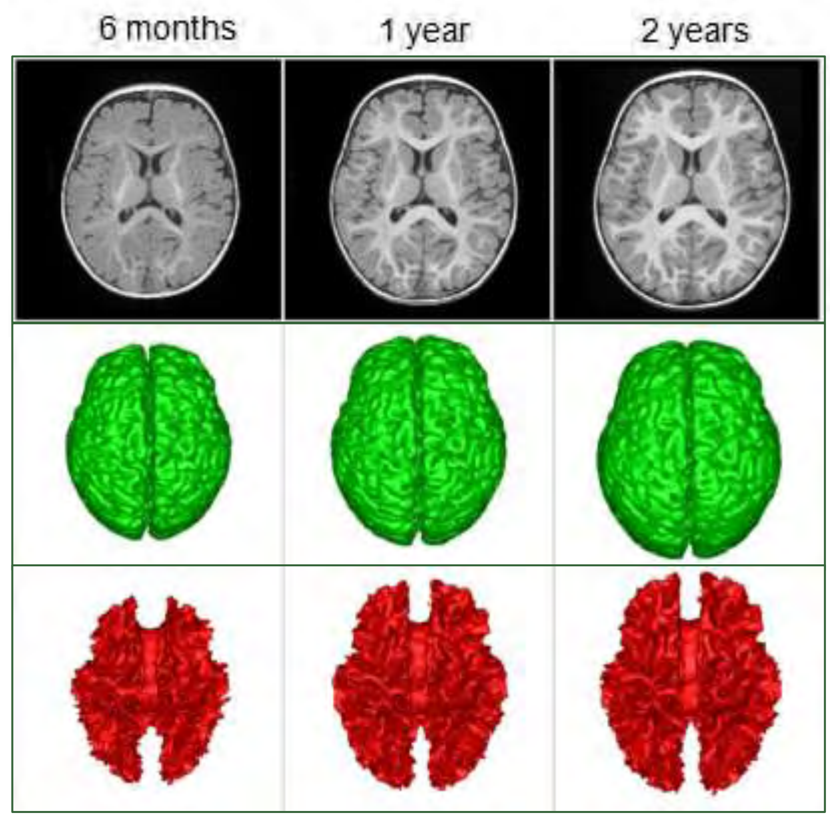

ACE-IBIS NIH Study: UNC (PI), McGill, Seattle, WU, CHOP, <u>UNC</u> & <u>Utah (Image Analysis)</u>

Brain enlargement in autism starts at year 1.

Why? What? Effect?: Longitudinal MRI/DTI study w. >1250 MRI/DTI

Better understanding → Early intervention to improve outcome

Longitudinal Shape Regression

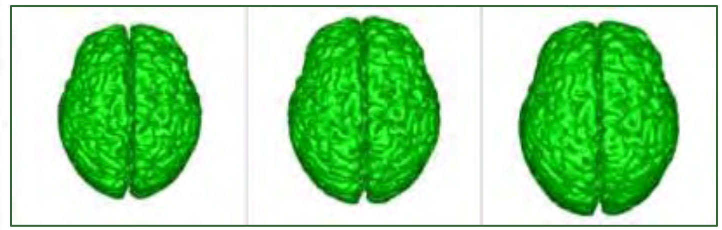

movie

Durrleman, Fishbaugh, Gerig,
MICCAI 2011, MICCAI 2012

4D Shape Regression

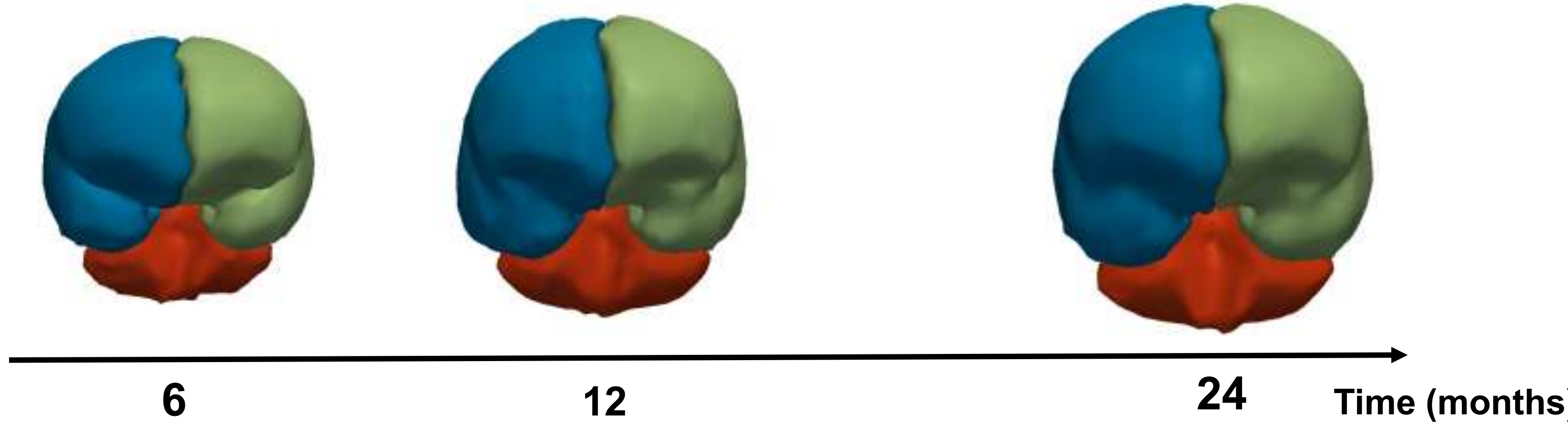

From discrete 3D shapes (6m,12m,24m) to continuous 4D shape model

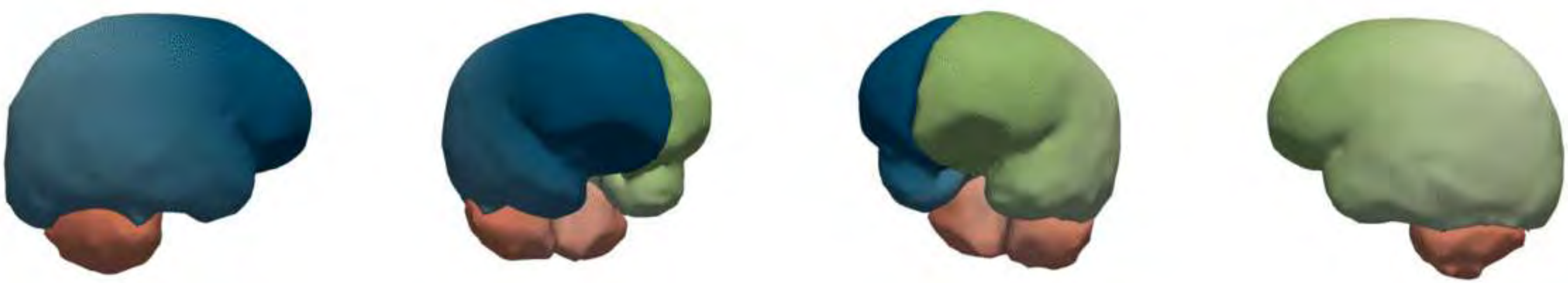

Fishbaugh, Durrleman, Gerig, MICCAI 2011, 2012

Individual 4D Growth Profiles

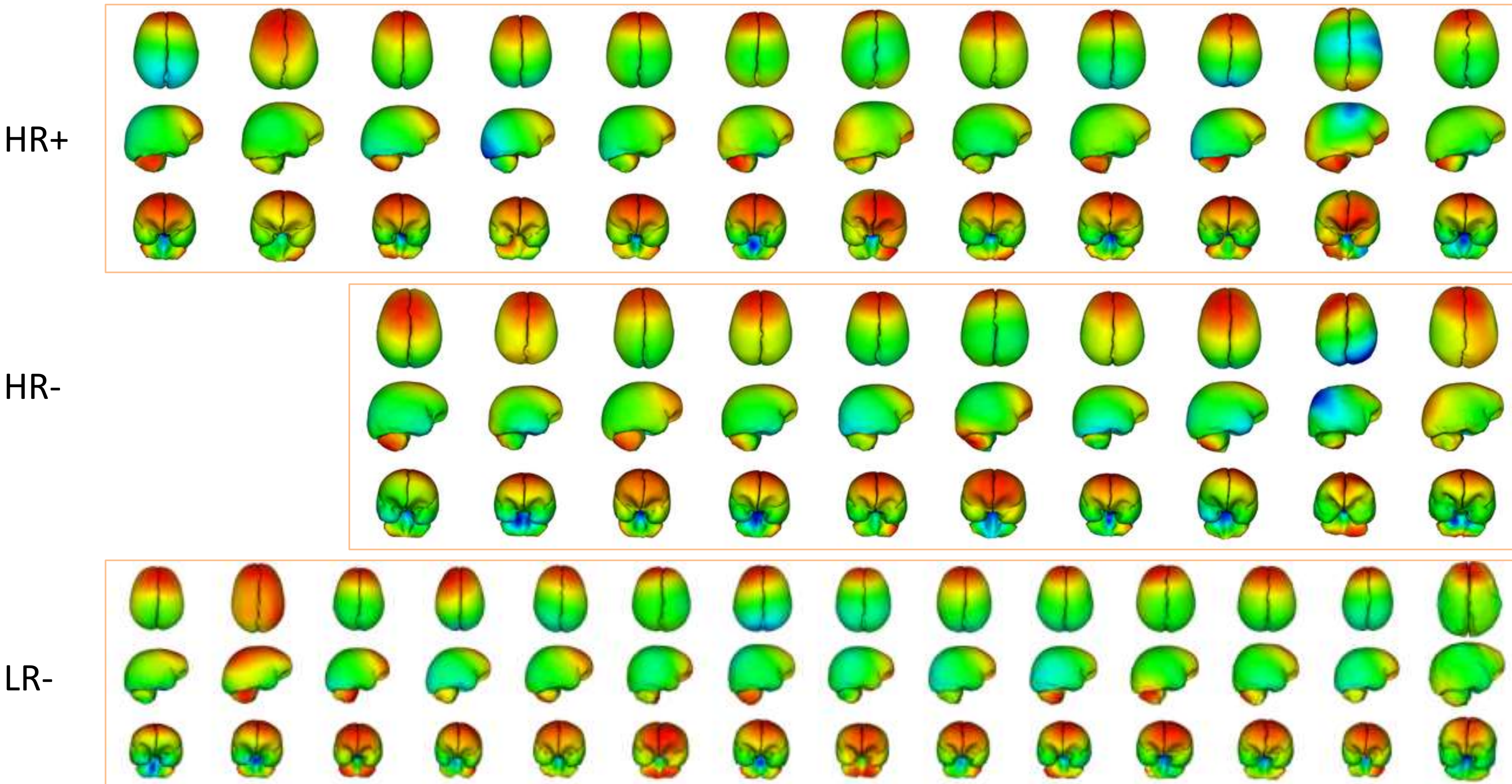

4D Shape Modeling and Statistics

Conventional approach

Temporally discrete measurements

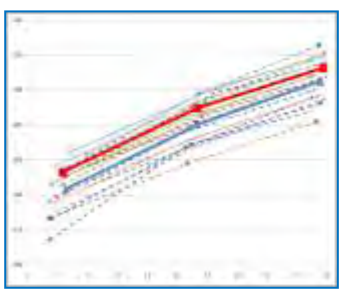

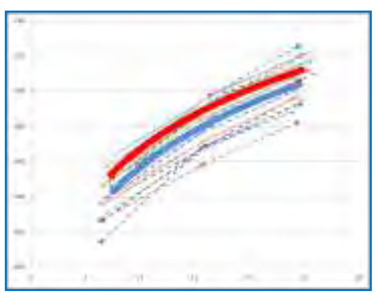

- Fit statistical model through discrete data, 1D regression not biologically motivated.
- Regression model adjusted to data.

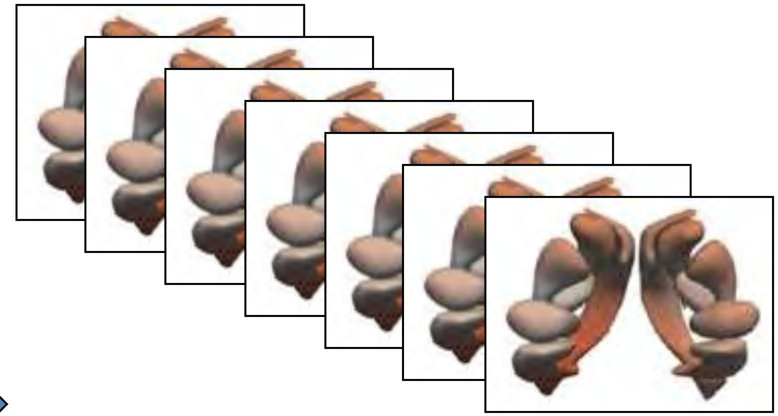

Temporally continuous shape regression

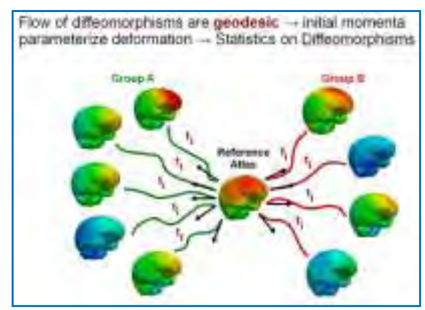

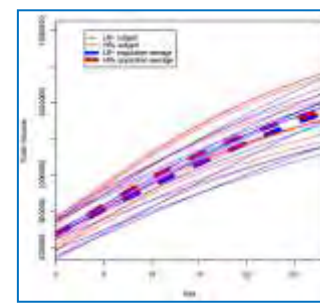

- Statistics on 4D shape trajectories.
- Measurements of interest continuous in time, can be sampled at arbitrary time points.

Longitudinal Shape Modeling

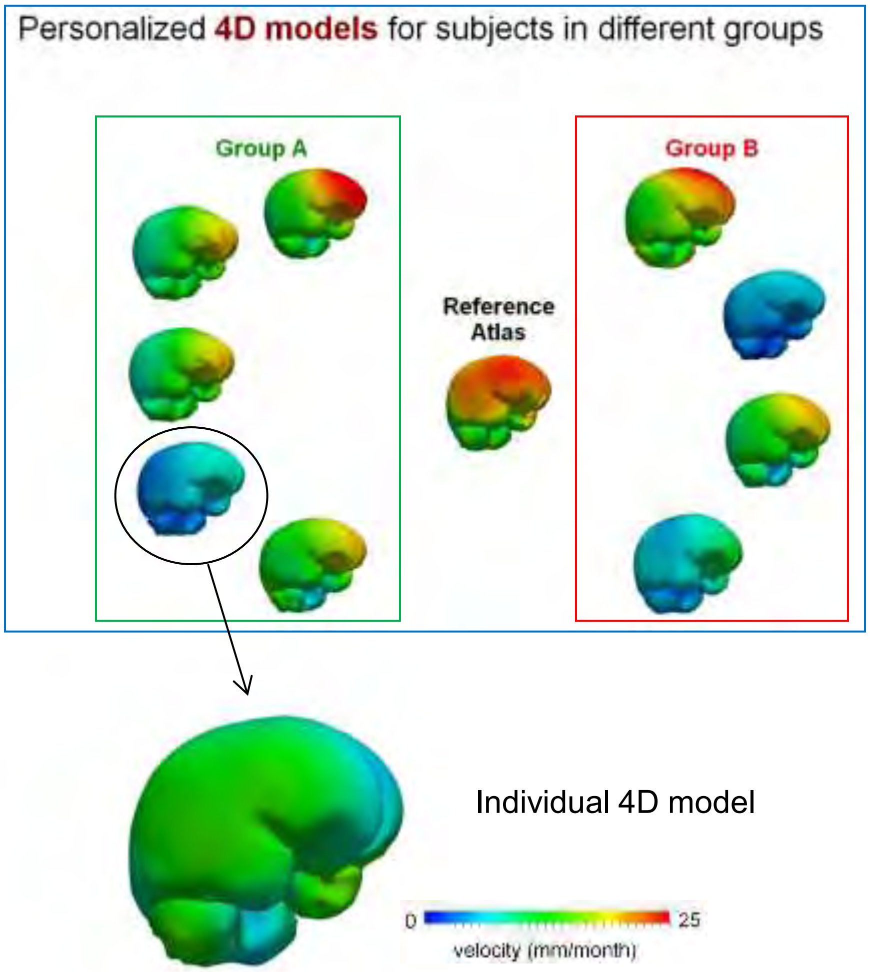

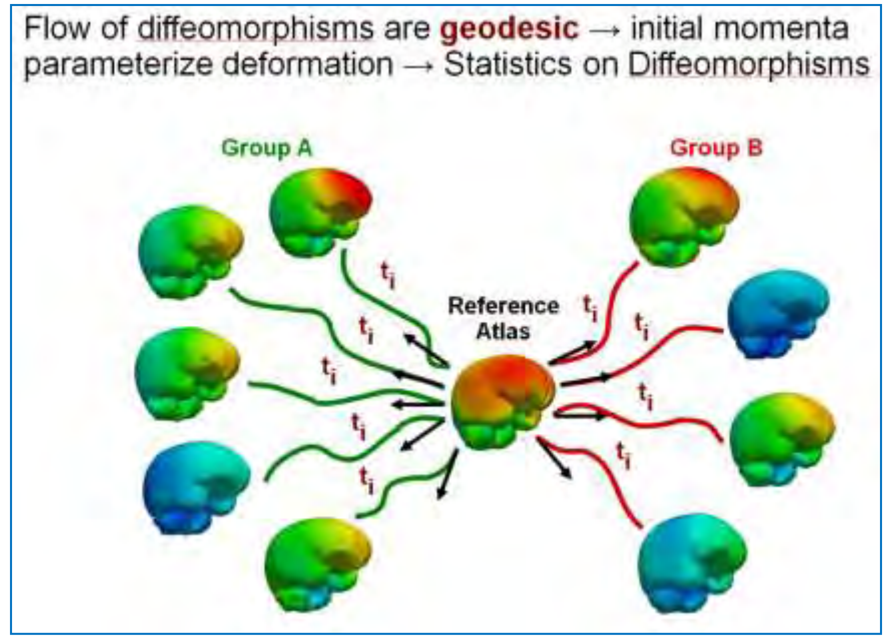

Work in progress: Stats of 4D growth profiles

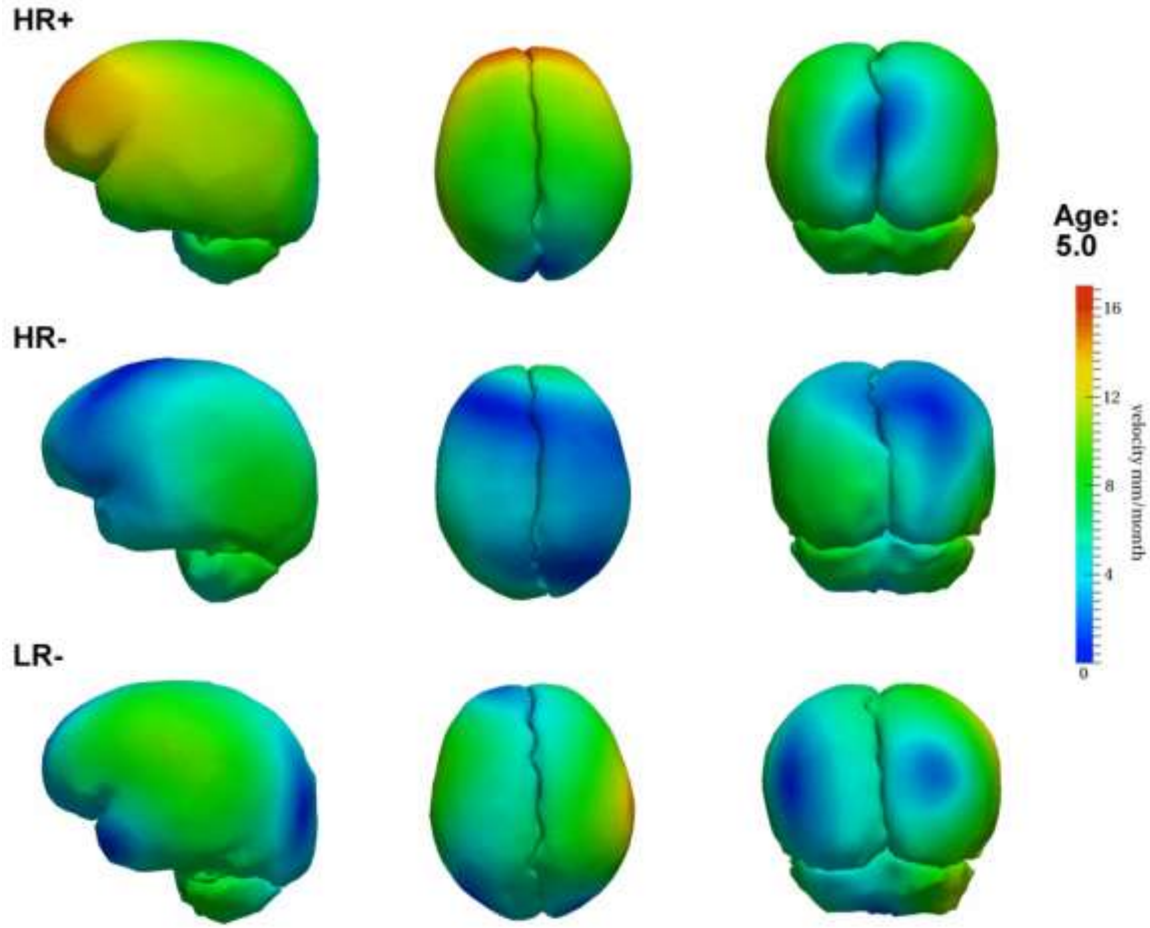

Autism Research Collaboration UNC (Piven, Hazlett)

HR+: High risk infant ADOS pos.

HR-: High risk infants ADOS neg.

LR-: Low risk healthy infants

Autism Research Collaboration ACE-IBIS (PI J. Piven, UNC)

Quantification of spatio-temporal population differences

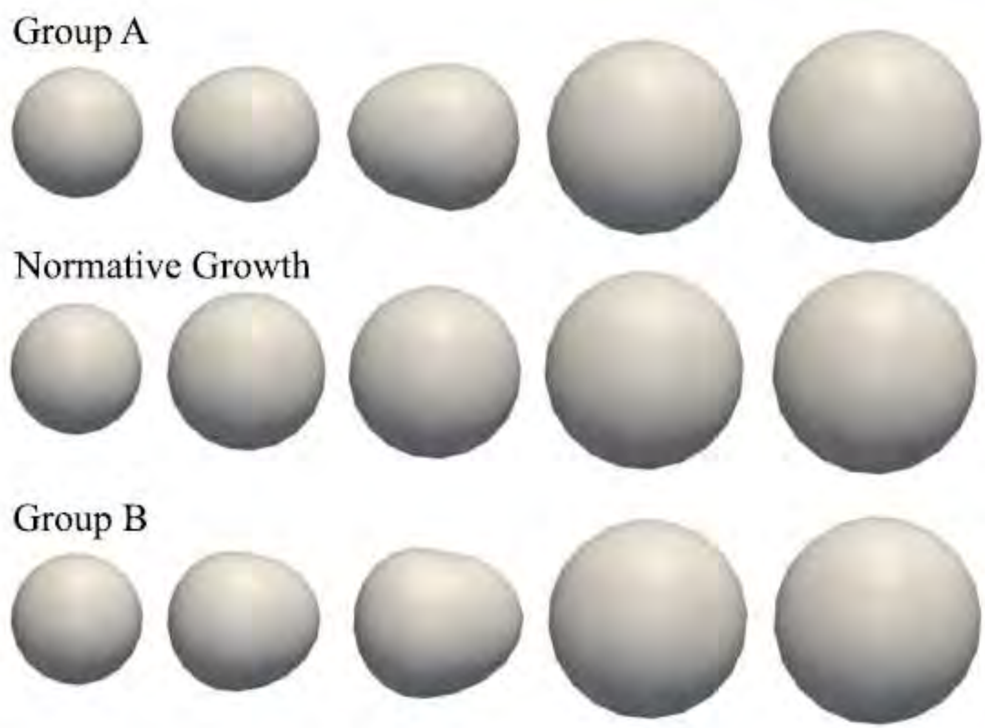

Fig. 2. The synthetic shape database with observations at 6, 10, 12, 18, and 24 months. **Top**: Typical shape observations for a subject from group A. **Middle**: The normative growth scenario. **Bottom**: Typical shape observations for a subject from group B.

Fishbaugh et al., MICCAI'12

Quantification of spatio-temporal population differences

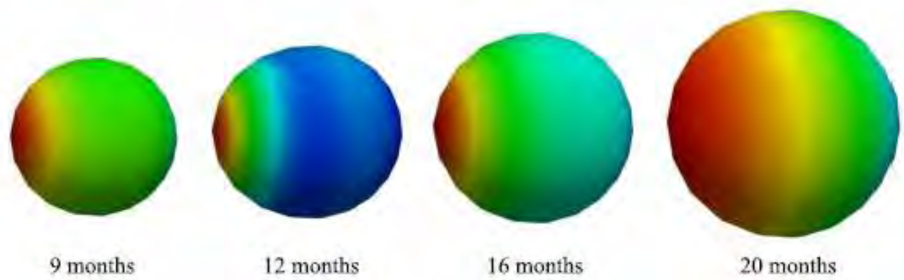

Fig. 3. The first major mode of deformation from PCA (mean plus one standard deviation) at selected time points for group A. Color indicates the displacement from the mean shape. The variability in the protuberance is clearly captured.

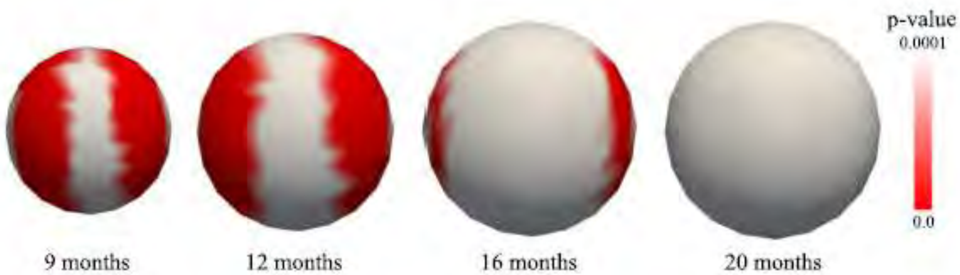

Fig. 4. Significant differences in magnitude of momenta between group A and B at several time points, with p-values displayed on the surface of the reference atlas.

Fishbaugh et al., MICCAI'12

First mode of deformation from **PCA** per age group

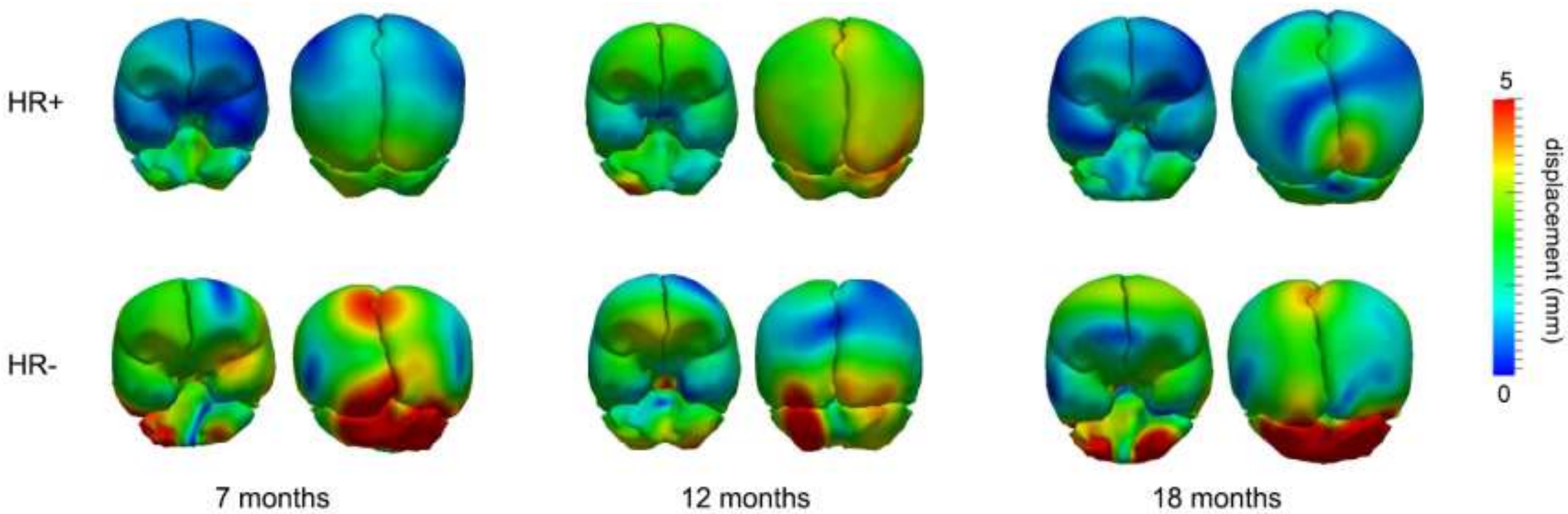

Hypothesis testing → **no significant** differences in magnitude of initial momenta

Study: Brain scans detect early signs of autism

Link to CBS News

comments 3 | Like 66 | Tweet 57 | +1 8 | Share 6 | More +

THE AMERICAN JOURNAL OF PSYCHIATRY

Home | Current Issue | All Issues | Topics

The American Journal of Psychiatry, VOL. 169, No. 6

ARTICLES | June 01, 2012

Differences in White Matter Fiber Tract Development Present From 6 to 24 Months in Infants With Autism

Jason J. Wolff, Ph.D.; Hongbin Gu, Ph.D.; Guido Gerig, Ph.D.; Jed T. Elison, Ph.D.; Martin Styner, Ph.D.; Sylvain Gouttard, M.S.; Kelly N. Botteron, M.D.; Stephen R. Dager, M.D.; Geraldine Dawson, Ph.D.; Annette M. Estes, Ph.D.; Alan C. Evans, Ph.D.; Heather C. Hazlett, Ph.D.; Penelope Kostopoulos, Ph.D.; Robert C. McKinstry, M.D., Ph.D.; Sarah J. Paterson, Ph.D.; Robert T. Schultz, Ph.D.; Lonnie Zwaigenbaum, M.D.; Joseph Piven, M.D.; the IBIS Network

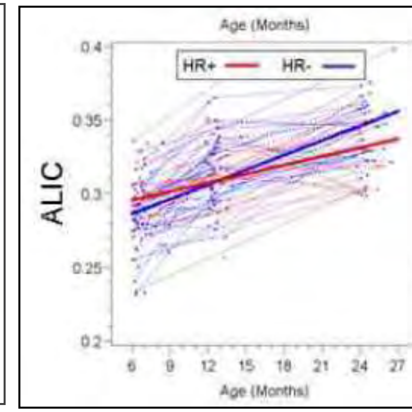

Researchers See Differences in Autism Brain Development as Early as 6 Months

AUTISM SPEAKS
It's time to listen.

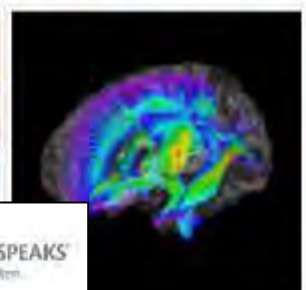

Scientists created 3D images of major brain pathways in infants at high risk for developing autism. [Credit: UNC]

The defining features of autism—hampered communication, social challenges and repetitive actions—may not become obvious until after a baby's first birthday. But the changes in brain development that underlie these behaviors may be detectable much earlier. In a new study, researchers found clear differences in brain communication pathways starting as early as 6 months and continuing through 2 years of age in children who were later diagnosed with autism spectrum disorder (ASD). The findings appear online today in the *American Journal of Psychiatry*.

Study Suggests Pre-Autism Brain Differences In Six Month Olds

redOrbit
YOUR UNIVERSE ONLINE

PREDICT-HD

Search for noninvasive biomarker with imaging…

- Symptomatic HD imaging findings
  - Atrophied caudate and putamen
  - Disproportionate loss of white matter
- Prodromal HD imaging findings
  - Striatal atrophy correlates with:
    - Neurological impairment
    - Poorer performance on cognitive assessments
    - Years to motor symptom onset

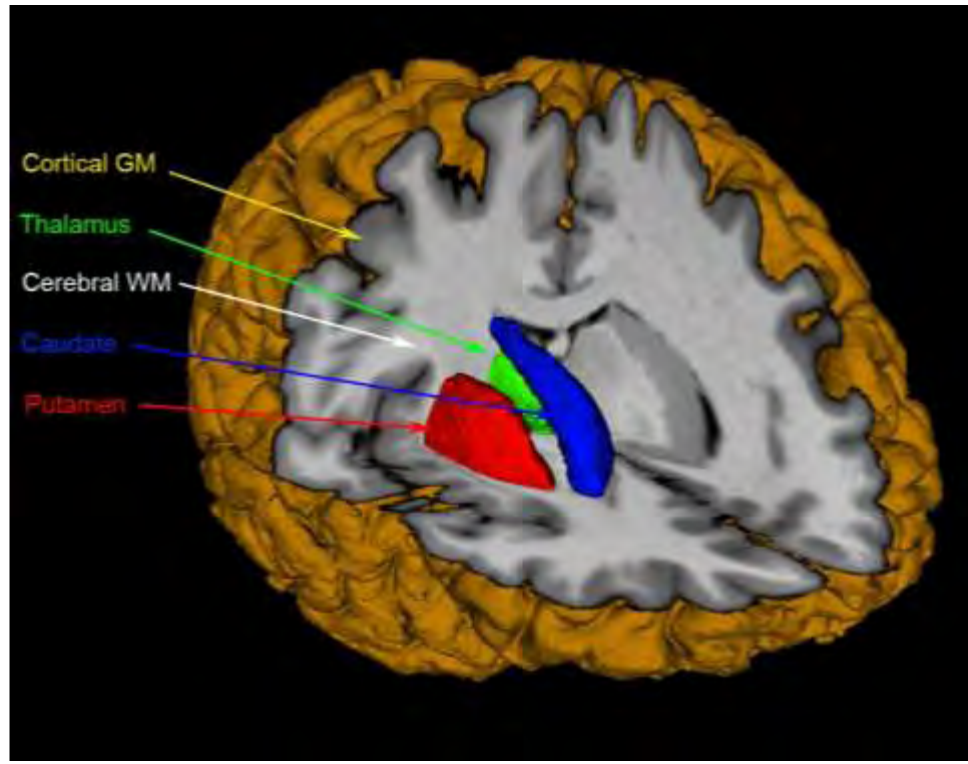

Courtesy Jane Paulsen, Hans Johnson, U-Iowa

Purpose: Huntington's Disease

What is Huntington's disease (HD)?

Etiology

- Progressive autosomal-dominant, polyglutamine disease
- Mutation: Expanded trinucleotide CAG-repeat in huntingtin gene [77]

Signs and symptoms: Motor, cognitive, and psychiatric disturbances

Diagnosis

- Usually made in mid-life (35-42)
- Onset of motor symptoms with positive family history [76]
- Confirmed with genetic testing (expanded CAG-repeat)
- Radiographic feature: Prominently decreased striatum (caudate and putamen) at mid-stage

Treatment: Symptomatic only

Prognosis: Duration of disease is 17-30 years after diagnosis, depending on CAG-repeat length

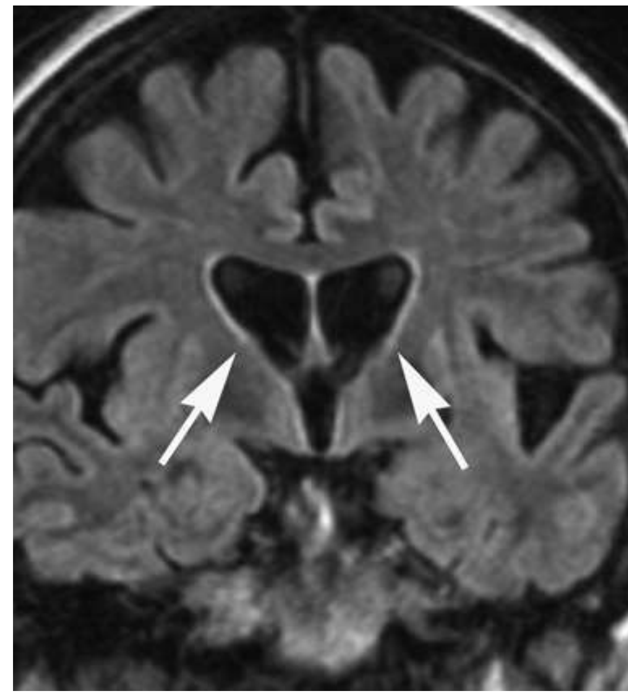

Purpose: HD treatment

How can we help HD patients?
- Present: Symptomatic treatment (no cure)
- Future: Treatment for pre-symptomatic or **prodromal HD patients** that slow or stop progression **before** debilitating symptoms start

What do prodromal treatment studies need?
- Method to **monitor treatment efficacy** when visible symptoms are not present
- **Solution: Use noninvasive biomarker**
  - Representable on a continuous scale
  - Distinguishes individuals by disease state

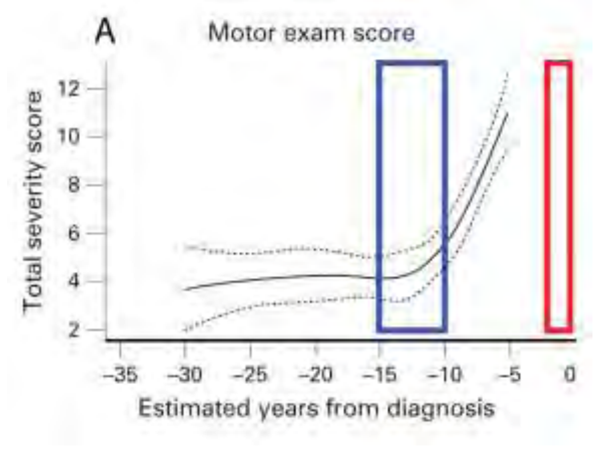

PREDICT-HD

Huntington's Disease Imaging Study:

- Neurodegenerative, progressive disease
- Longitudinal imaging (MRI)
- Subtle changes over time
- <u>Atrophied</u> caudate and putamen
- Processing: Longitudinal shape regression

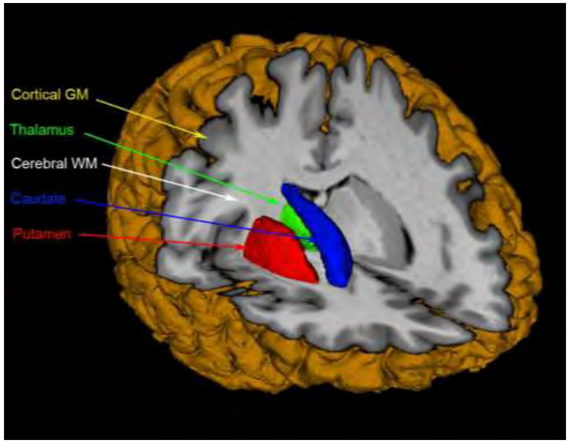

Huntington's Disease: Joint analysis of sets of anatomical structures

Data: Iowa Huntington Disease (HD) study (NAMIC)

Goal: Prediction of onset of HD from longitudinal preclinical imaging

Clinical Application: Neurodegeneration in Huntington's Disease

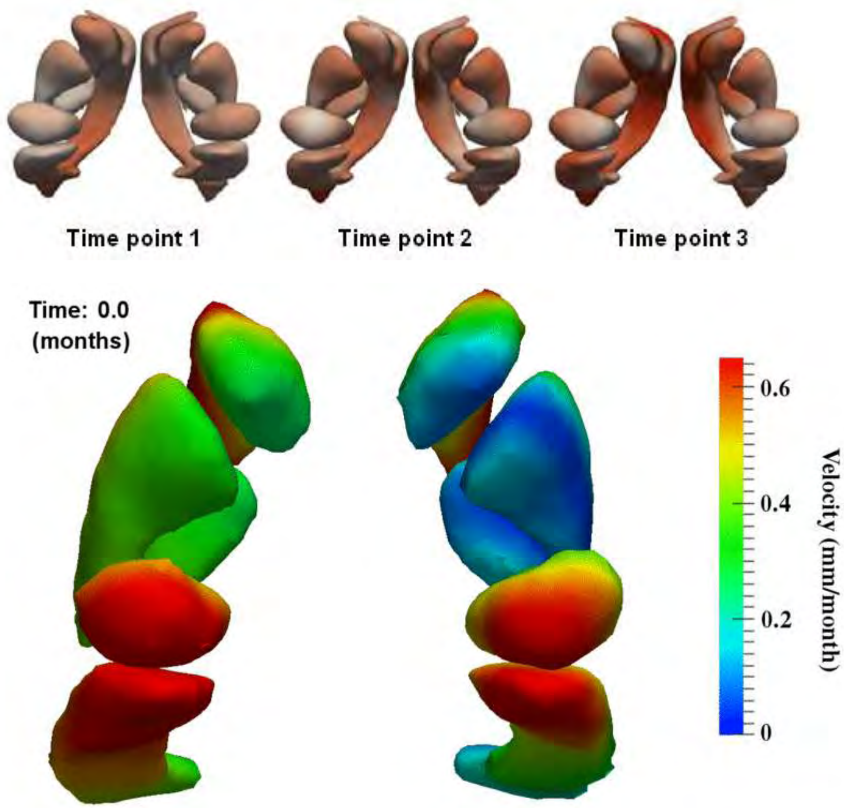

Continuous individual subjects' growth models

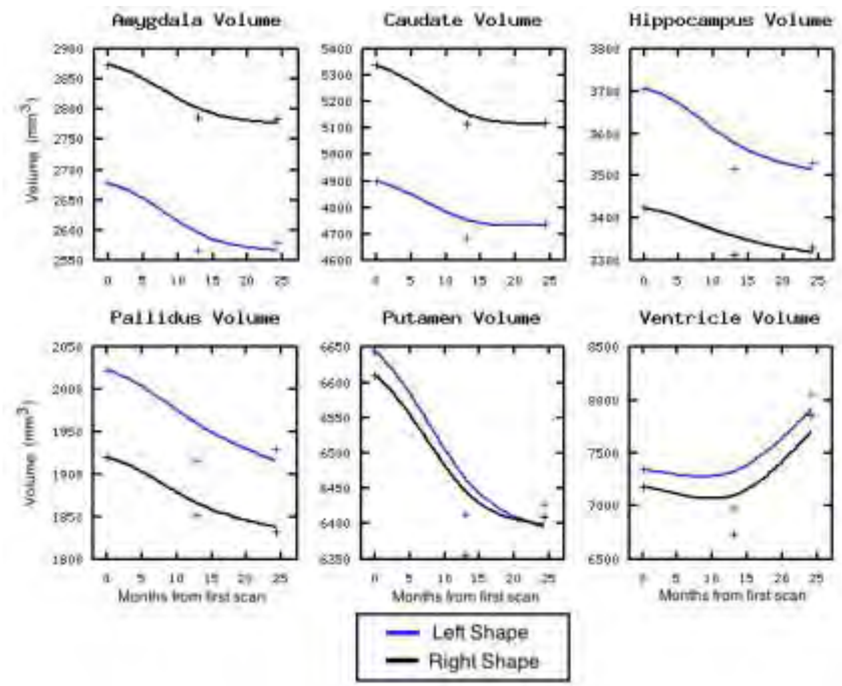

Quantitative information derived from 4-D shapes

James Fishbaugh et al., Utah

Degeneration of Caudate Volume by Clinical Risk Groups

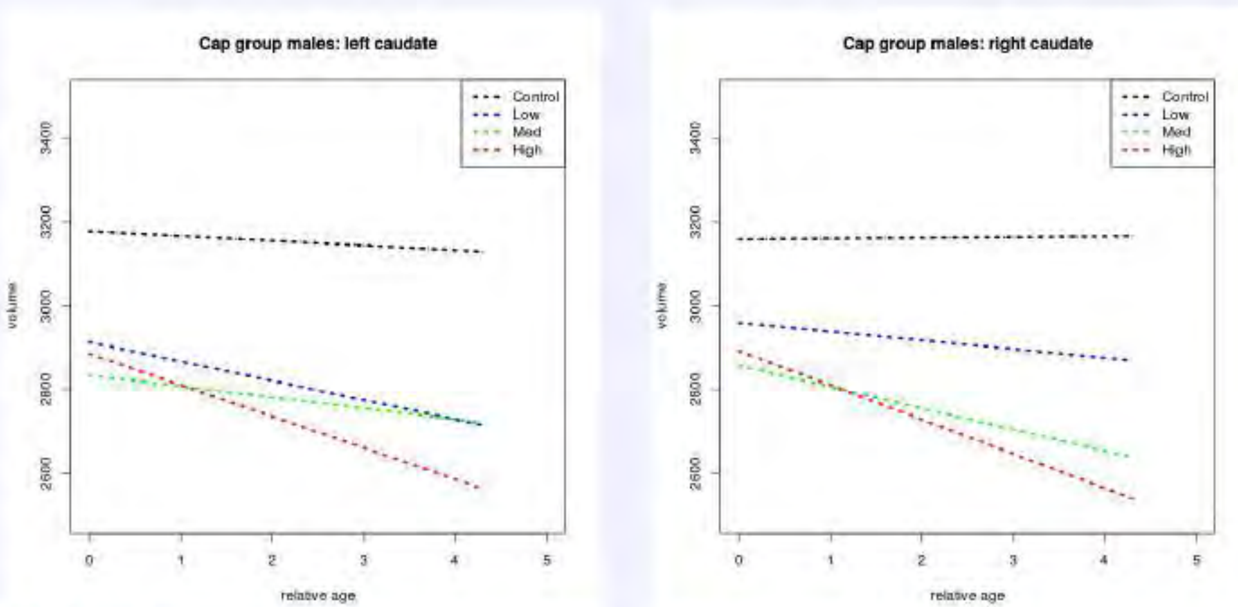

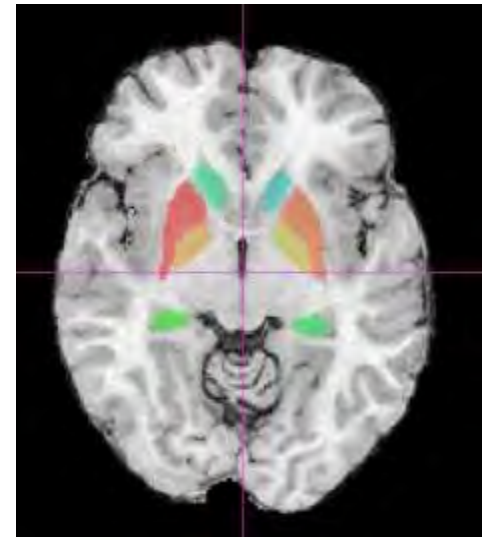

<u>Model:</u>

$$\text{volume} = \beta_0 + \beta_1\,(\text{relAge}) + \beta_2\,(\text{cap group}) + \beta_3\,(\text{relAge} * \text{cap group})$$

Muralidharan, Fletcher, Fishbaugh, Gerig, MICCAI 2014

Personalized/Individual Profiles: Problem of Variability in 3D Segmentation

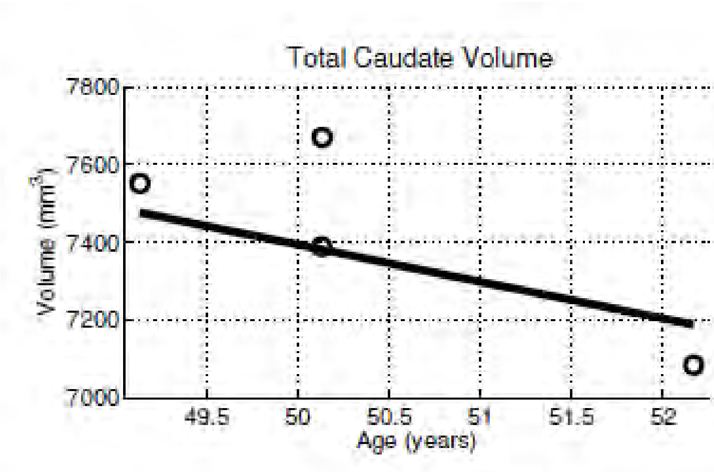

Volumes from one subject

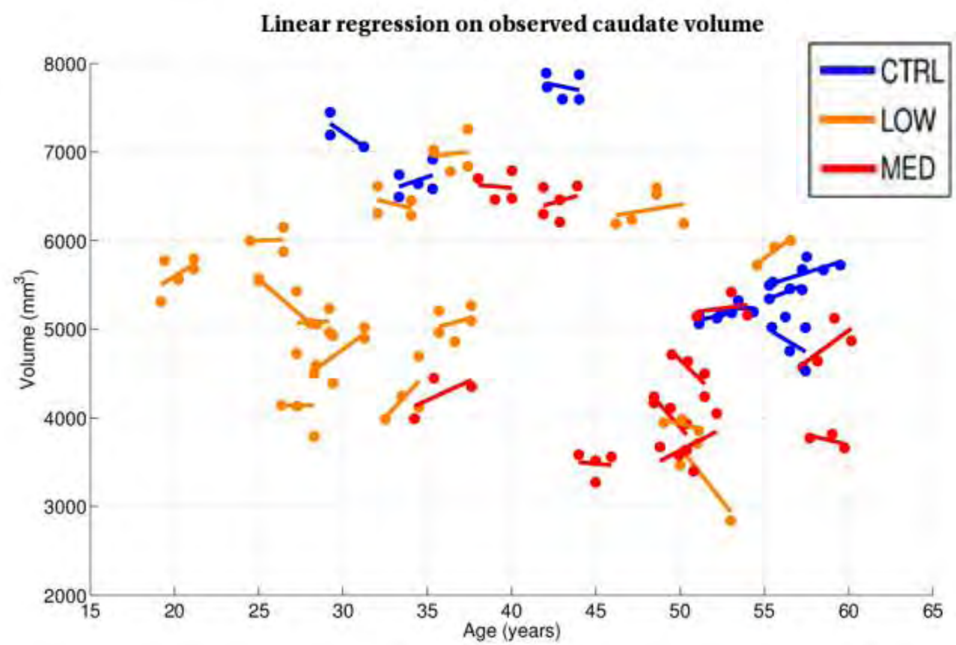

Volumes from multiple subjects with varying disease burden

HD: Joint 4D Modeling of subcortical structures

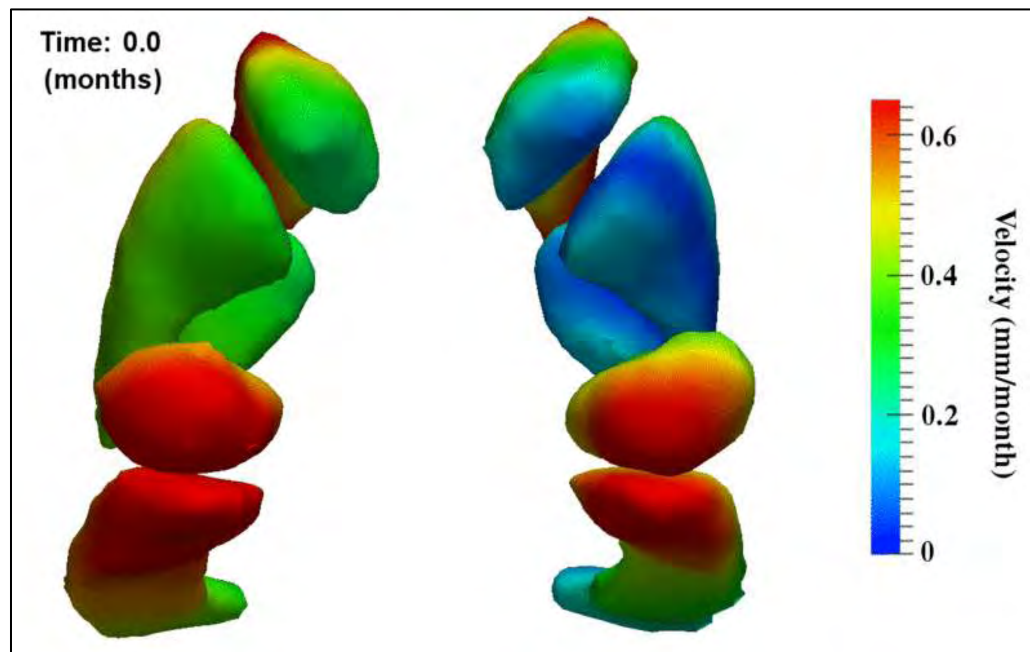

Subject-Specific Shape Modeling

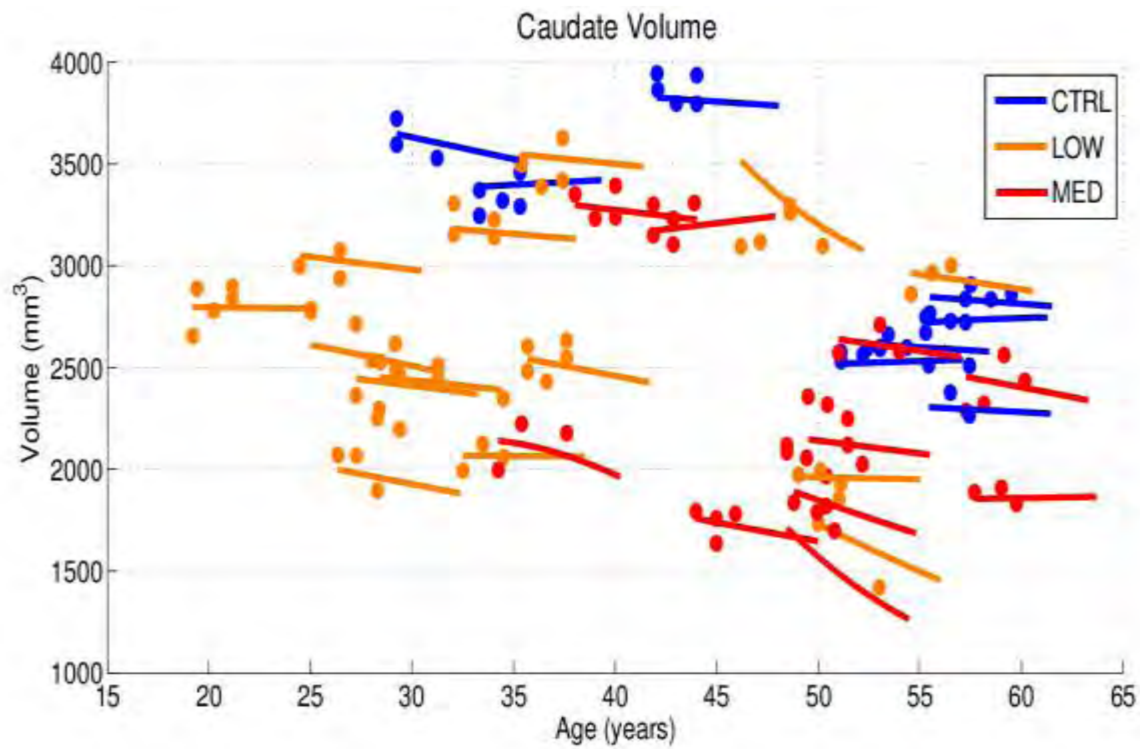

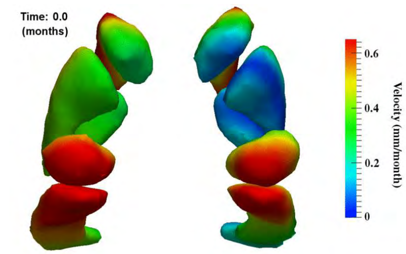

	CTRL	LOW	MED
Caudate	0.78%	4.22%	6.25%
Hippocampus	0.65%	1.09%	2.18%
Acumben	0.11%	2.13%	3.09%

Table 1: Average percentage volume decrease for caudate, hippocampus, and acumben.

- Caudate volume for 32 subjects (3 time pts) extracted <u>after shape regression</u>.
- Observed volumes shown as circles, highlighting the noise in segmentation.
- Our shape regression estimates <u>consistent shape trajectories </u>by considering all shapes simultaneously.
- **Result: Improved subject-specific modeling of neurodegeneration.**

Muralidharan, Fishbaugh et al, MICCAI 2014

Longitudinal Segmentation

Huntington's Disease study (30 CTRL, 16 LOW, 24 MED, 14 HIGH)

- Models estimated with subcortical shape complexes (12

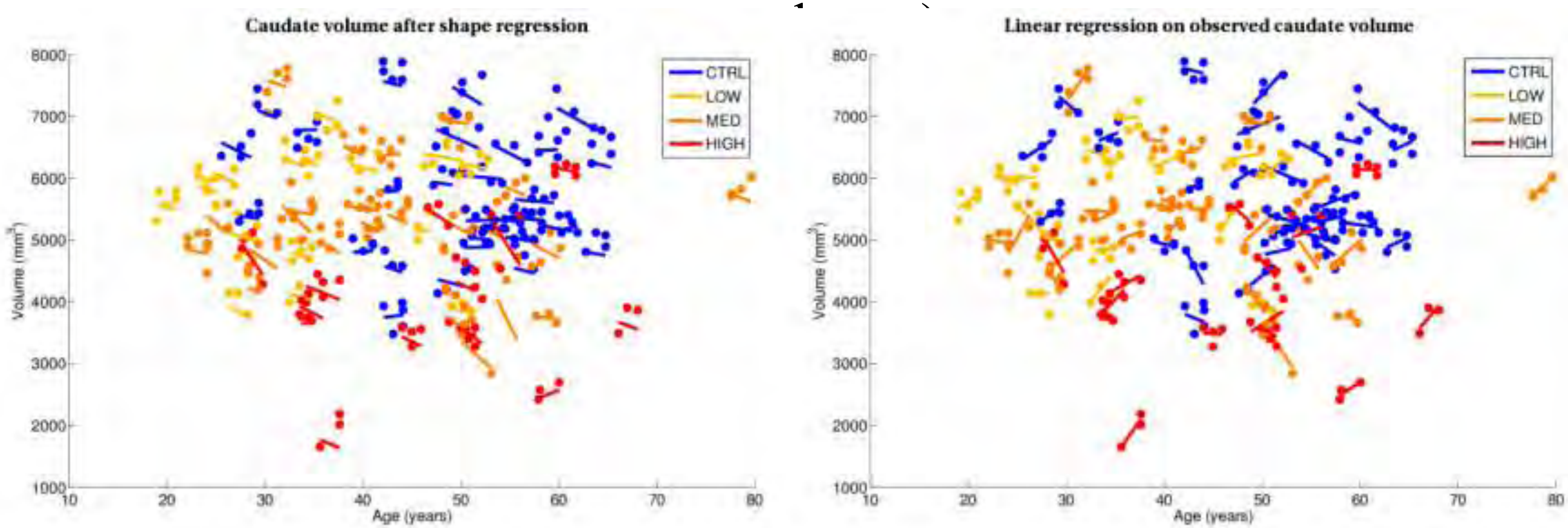

	PERCENT VOLUME CHANGE FROM SHAPE REGRESSION				PERCENT VOLUME CHANGE FROM LINEAR REGRESSION			
	CTRL	LOW	MED	HIGH	CTRL	LOW	MID	HIGH
CAUDATE	-1.41	-2.11	-3.39	-4.84	0.01	1.31	1.00	1.05
PUTAMEN	-3.11	-5.01	-5.42	-6.74	0.29	-0.09	0.06	0.01
HIPPOCAMPUS	-1.55	-1.38	-1.34	-1.55	0.32	0.93	1.23	0.96
THALAMUS	-1.68	-2.47	-1.19	-1.93	0.66	0.49	-0.06	0.40
ACUMBEN	-0.58	-1.52	-1.39	-2.67	-0.04	-2.81	-0.01	1.36
PALLIDUS	-3.82	-5.49	-5.51	-6.76	0.29	-0.25	-0.52	-2.43

GEODESIC REGRESSION OF IMAGE AND SHAPE DATA

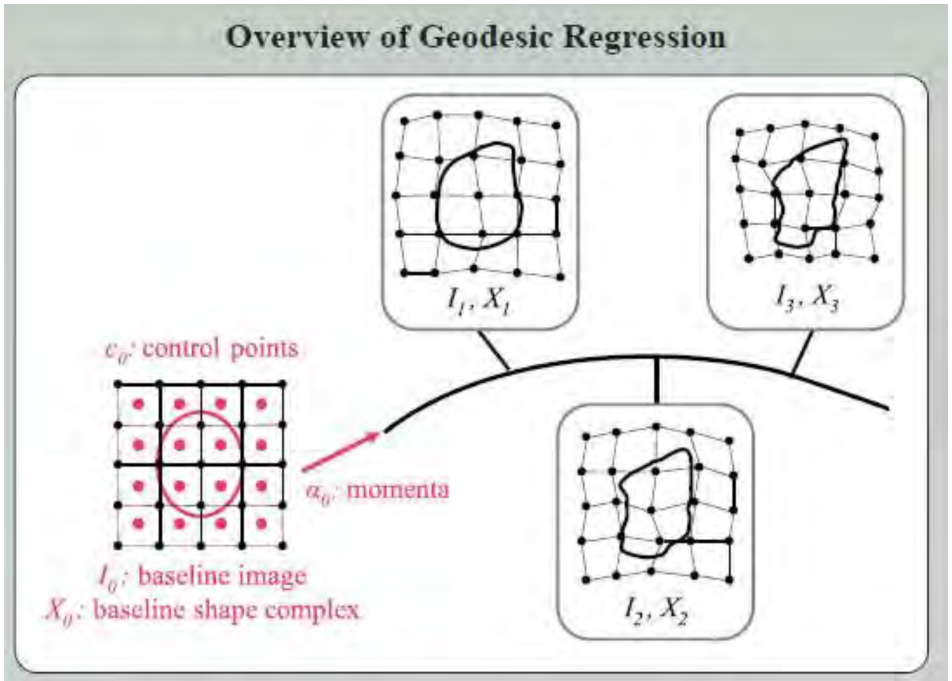

Control Point Parameterization of Diffeomorphisms

$$\begin{cases} \dot{c}_i(t) = \sum_{p=1}^{N_c} K(c_i(t), c_p(t))\alpha_p(t) \\ \dot{\alpha}_i(t) = -\sum_{p=1}^{N_c} \alpha_i(t)^t \alpha_p(t) \nabla_1 K(c_i(t), c_p(t)) \end{cases}$$

Trajectory of particle at point x given by integral curve of

$$\frac{\partial \phi(x,t)}{\partial t} = v(x,t) = \sum_{p=1}^{N_c} K(x, c_p(t))\alpha_p(t)$$

$$\phi(x,0) = 0$$

Fishbaugh et al, ISBI 2014

GEODESIC REGRESSION OF IMAGE AND SHAPE DATA

Flow of Diffeomorphisms Deform Images and Shapes

Baseline image I_0 is deformed by flow of diffeomorphisms with trajectory

$$I(t) = I_0 \circ \phi(.,t)^{-1}$$

where the inverse flow satisfies the equation

$$\frac{\partial \phi(.,t)^{-1}}{\partial t} = -d\phi(.,t)^{-1} v(.,t)$$

Vertices of baseline shape complex concatenated into vector X_0 move at time t to

$$X(t) = \phi(X_0, t)$$

Regression Criterion

Trade off between matching observations and regularity of diffeomorphic flow

$$E(c_0, \alpha_0, I_0, X_0) = \sum_{t_i} \Big(\underbrace{D_I(I(t), I_{t_i})}_{\substack{\text{Image match} \\ \text{(L2-norm)}}} + \underbrace{D_S(X(t), X_{t_i})}_{\substack{\text{Shape match} \\ \text{(currents metric)}}} \Big) + \underbrace{\mathrm{Reg}(\phi)}_{\text{Regularity}}$$

Works with images alone, shapes alone, or any combination of both.

Fishbaugh et al, ISBI 2014

Subject-specific 4-D shape & image regression

Control 2yrs Interval

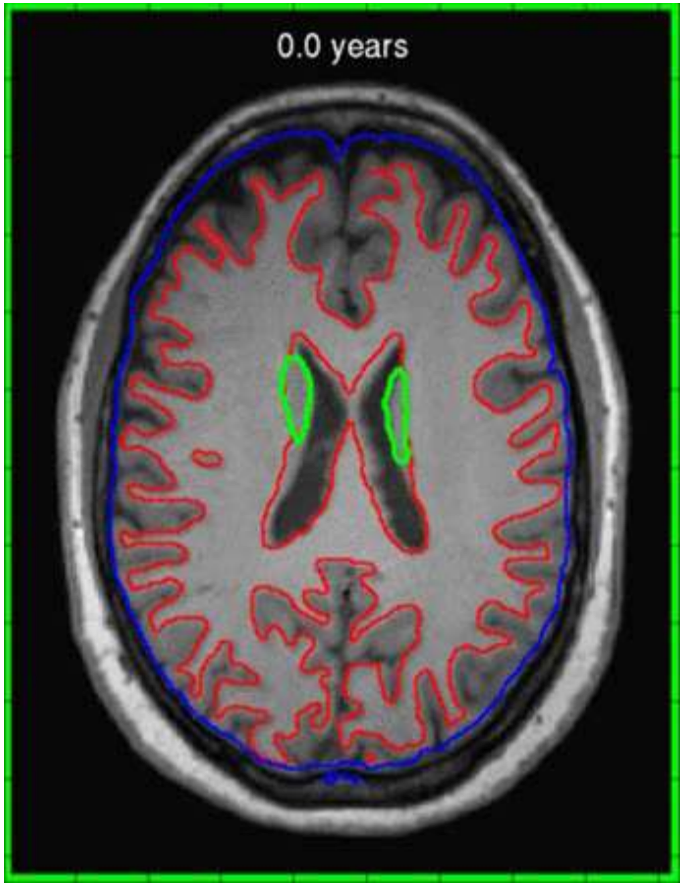

Huntington's D. 2yrs Interval

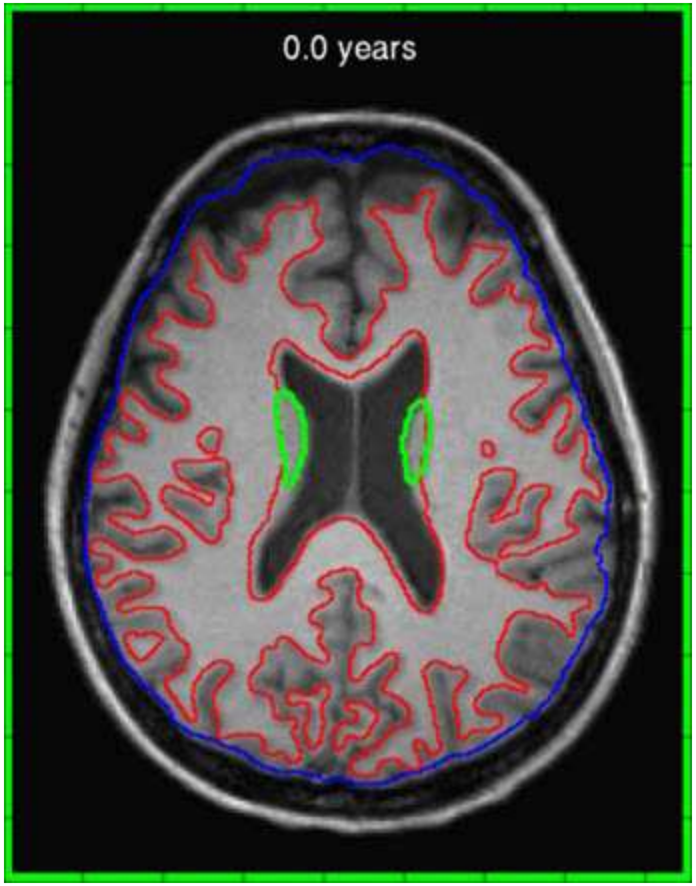

Fishbaugh et al., IPMI 2013

Huntington's Disease: Joint 4-D Modeling of Shapes and Images

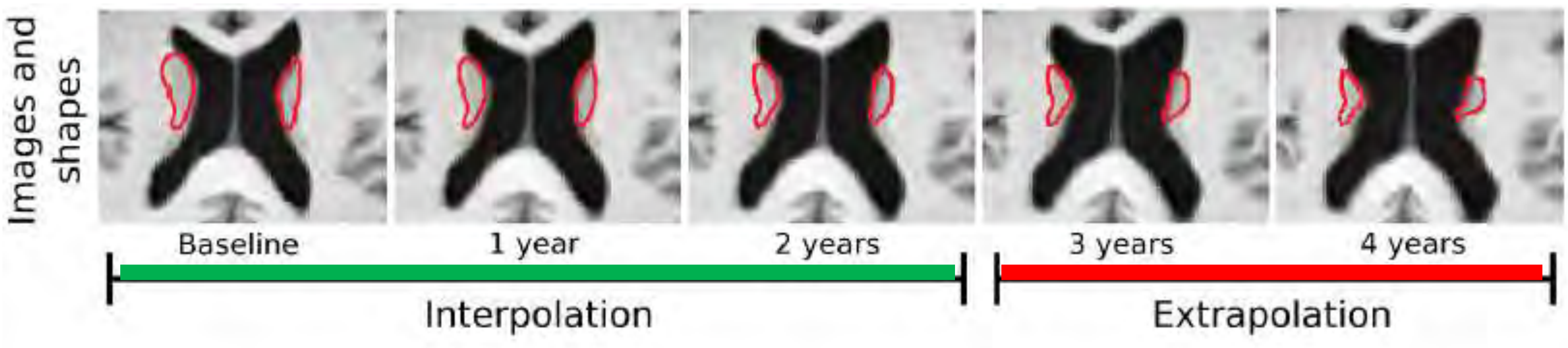

Single subject diagnosed with HD scanned at 58, 59, and 60 years of age.

- T1W images.
- Left/right caudate segmented and manually cleaned.
- Geodesic model can be used to *extrapolate* into the future.

Patient-specific 4-D shape & image regression

Control Extrapolated

HD Extrapolated

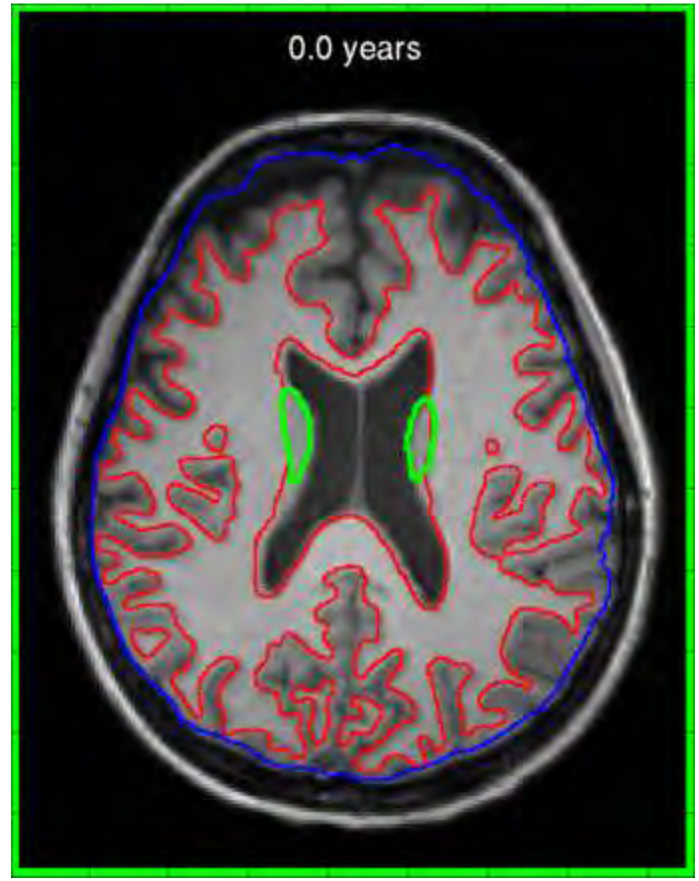

interpolation

extrapolation

time

Fishbaugh et al., ISBI '13, IPMI '13

Pediatric Brain Development

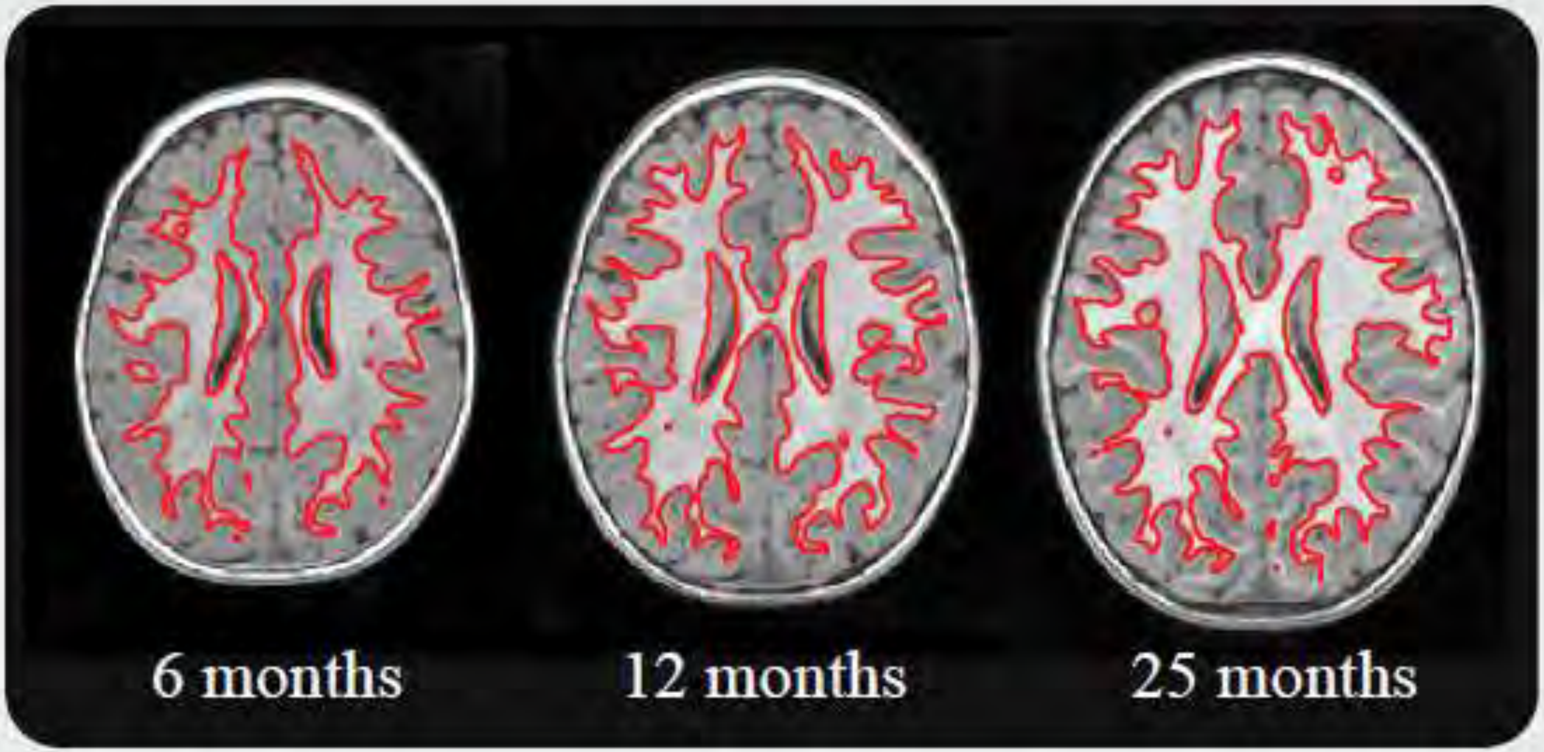

Longitudinal sequence of observed T1W images and white matter surfaces used for model estimation.

Pediatric Brain Development

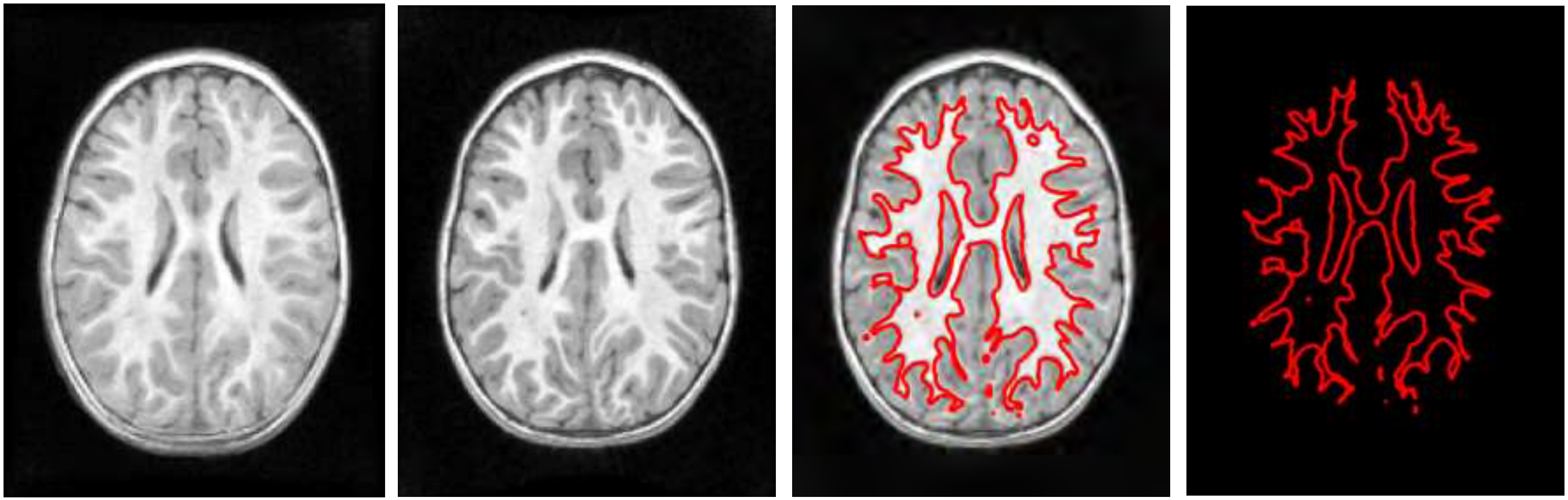

1) Estimation with images only
2) Estimation jointly but only showing image
3) Estimation jointly and showing both image and white matter
4) Estimation with white matter surfaces only

Pediatric Brain Development

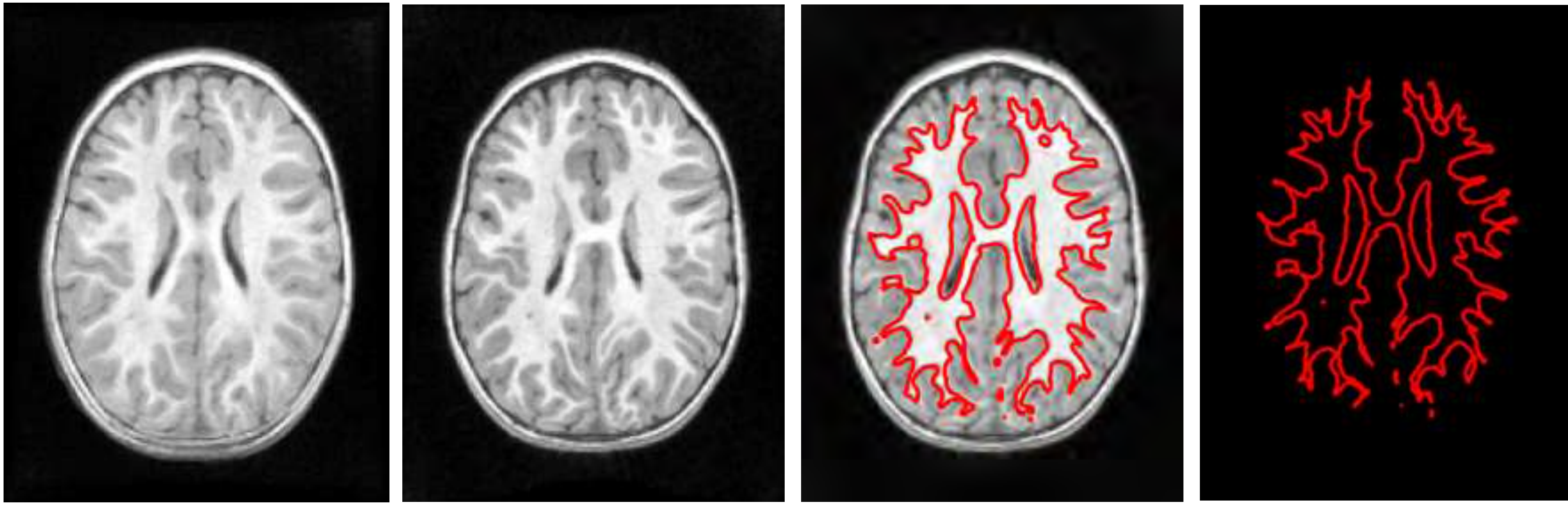

We present methodology for geodesic regression that jointly considers image and shape information in the (LDDMM) framework.

- Dense diffeomorphisms built using a control point formulation, decoupling deformation parameters from input object parameters (e.g., voxels, surface points).
- Our regression model seamlessly handles images and multi-object complexes consisting of points, curves, and/or surfaces in different combinations.
- Compared to image regression alone, shape data provides anatomical information that constrains the regression, especially in cases where images have low contrast, by placing larger weights on regions with anatomical importance.
- Compared to shape regression alone, image information provides data in areas where segmentations are not available, as well as providing context to regions surrounding anatomical objects.

Fishbaugh et al, ISBI 2014

Longitudinal Shape Modeling

Example mandibular surgery case (L. Cevidanes, NA-MIC ancillary grant).

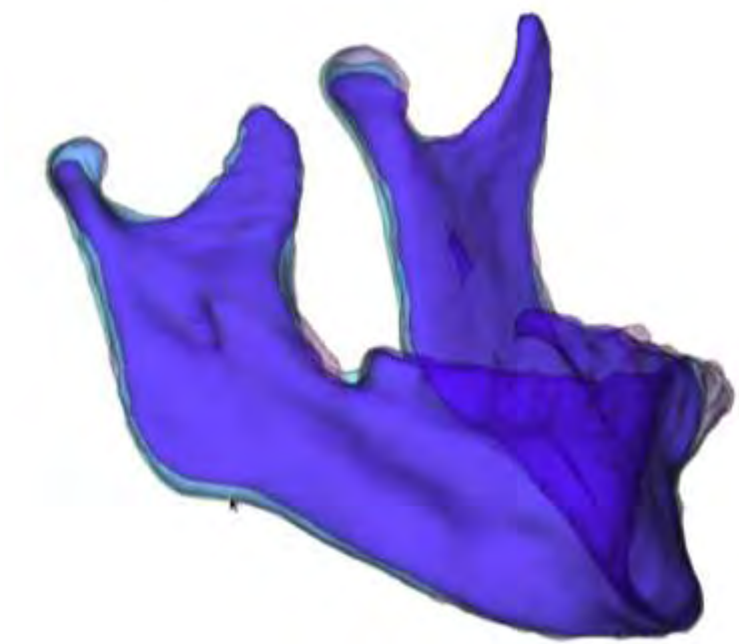

- V2- 16 years of age before jaw surgery in the upper jaw maxilla
- V6- 16 years of age 2 months post surgery
- V10- 18 years of age, 2 years post-surgery
- V12- 22 years of age, 6 years post-surgery

Qualitative analysis from overlay: Do we understand growth?

Longitudinal Shape Modeling

Example mandibular surgery case (L. Cevidanes, NA-MIC ancillary grant).
EXOSHAPE ACCEL Tool: Correspondence-free, controlled acceleration, no tuning, 20’ computing time

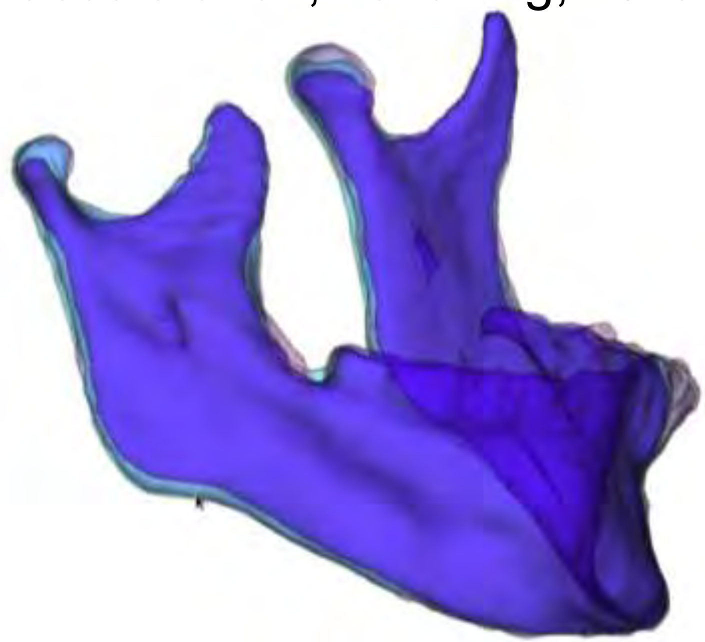

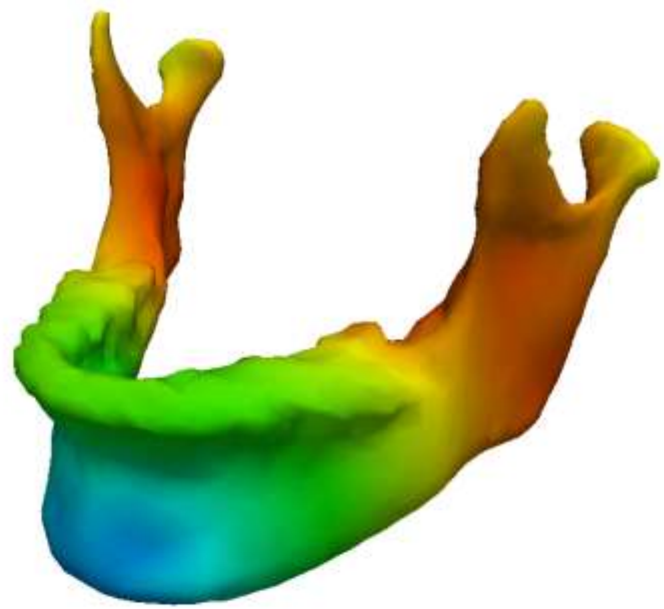

Color: speed:
blue = slow and red = fast

Application: Craniosynostosis

4D atlas from 350 full brain shapes (6 – 825 days)

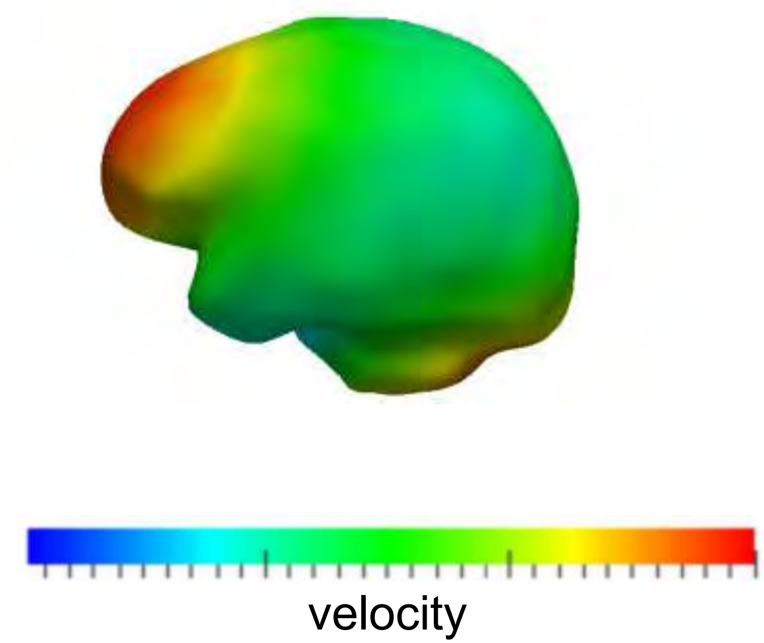

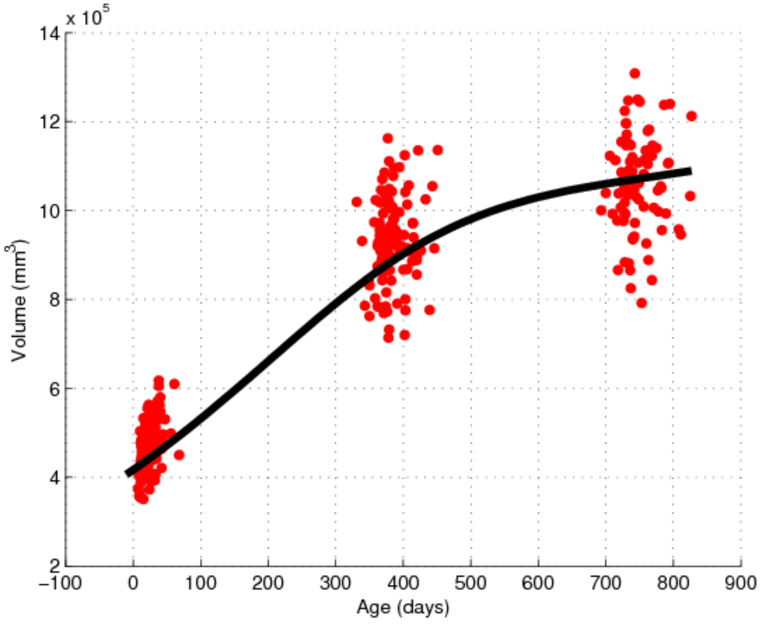

Paniagua, B. et al. 3D of brain shape and volume after cranial vault remodeling surgery for Craniosynostosis correction in infants. SPIE Medical Imaging 2013

Statistical Analysis of 4D Trajectories: Work in Progress

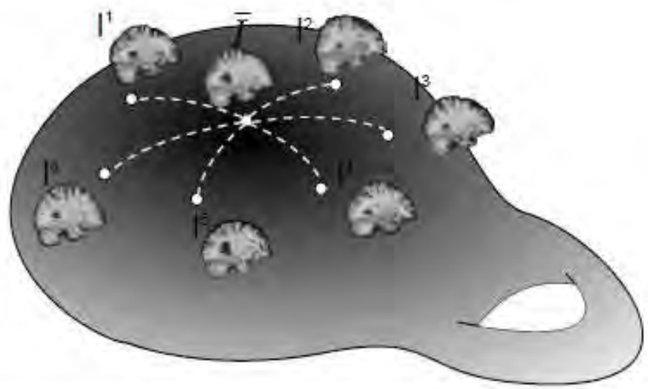

[3] Joshi et. al(2004), Beg et. al(2005)

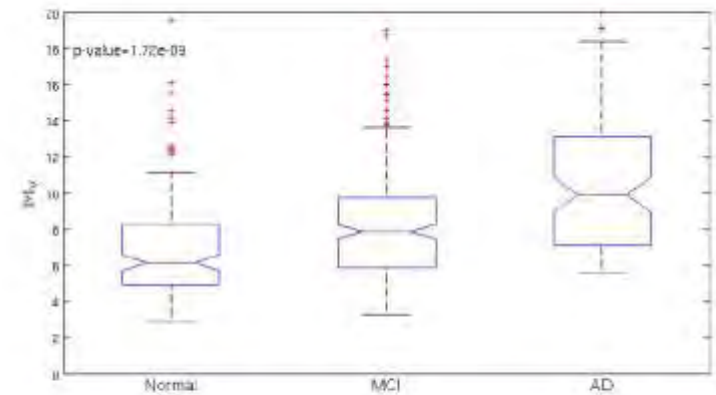

Group differences in rates of longitudinal atrophy in AD, MCI and Normal control.

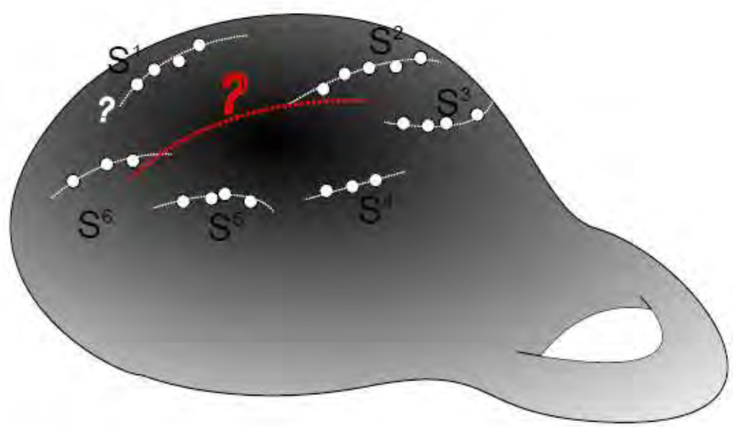

Repeated scans of anatomy over time and across population.

Group differences in rates of longitudinal change/atrophy in AD, MCI and Normal control.

Nikhil Singh et al., ISBI 2013, best paper award

Content

- Motivation Longitudinal Modeling
- Acceleration-Controlled Shape Regression
- Geodesic Shape Regression
- Driving Applications:
  - Early Brain Development in Autism
  - Huntington's Disease (HD)
  - Mandibular Growth
- Concept of Time Warp

4D Shape Analysis: Spatiotemporal Registration

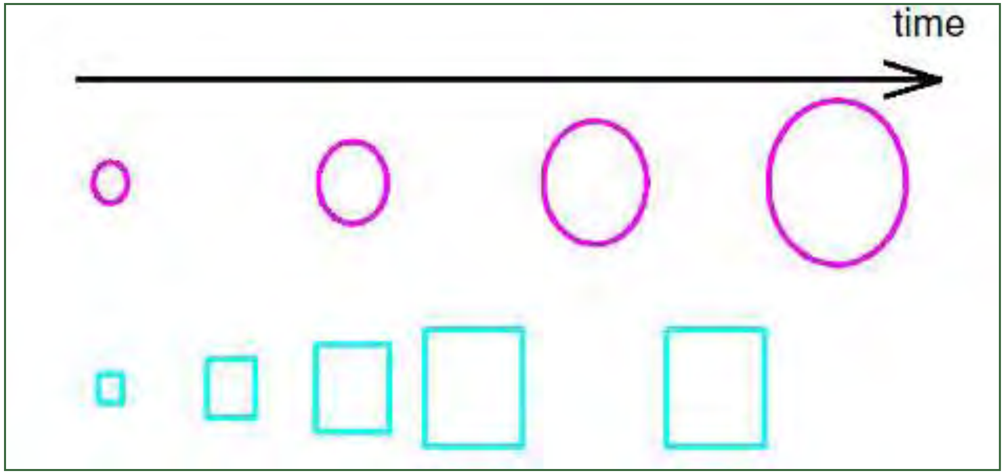

$$S(t) = \phi_t(M_0)$$

$$T(t) = \chi(S(\psi(t))), \text{ where}$$

χ : geometrical deformation

ψ : time change function

Comparing two evolutions:

Align shape trajectories:

$$S(t_i) \approx M_i$$

$$T(t_i) \approx N_i$$

Formalism captures:

- continuous regression: $\phi(t)$
- morphological change: χ
- change of growth speed: $\psi(t)$

Spatiotemporal variability analysis of longitudinal shape data, S. Durrleman, X. Pennec, A. Trouvé, G. Gerig, N. Ayache, MICCAI'10, IJCV 2012

4D Shape Analysis: Spatiotemporal Registration

Spatiotemporal Registration

$$J(\phi, \psi) = \sum_{t_j} \mathrm{d}\left(\phi\left(S(\psi(t_j))\right), T_{t_j}\right)^2 + \gamma_\phi \mathrm{Reg}(\phi) + \gamma_\psi \mathrm{Reg}(\psi)$$

$S(t)$: regression of red shapes
T_{t_j}: target's shapes
ϕ: geometrical deformation
ψ: time change function

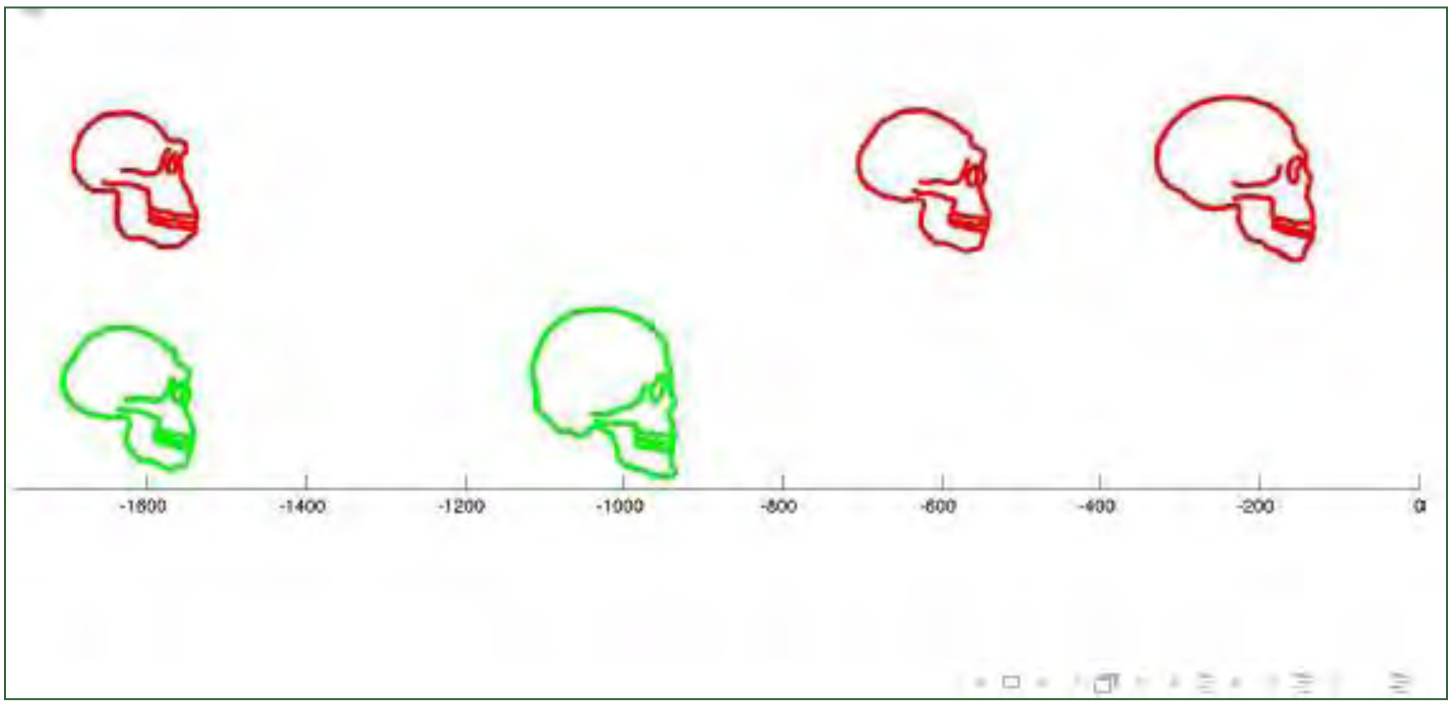

Spatiotemporal variability analysis of longitudinal shape data, S. Durrleman, X. Pennec, A. Trouvé, G. Gerig, N. Ayache

4D Shape Analysis: Spatiotemporal Registration

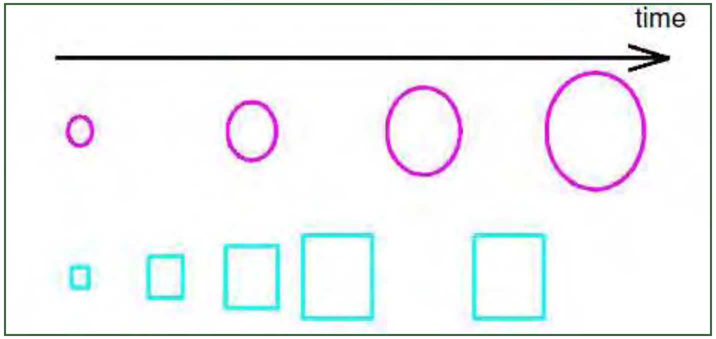

Spatiotemporal Variability:
- morphological changes
- change of growth speed

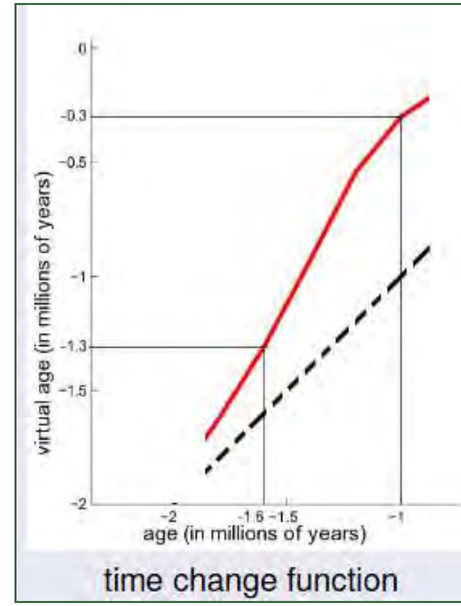

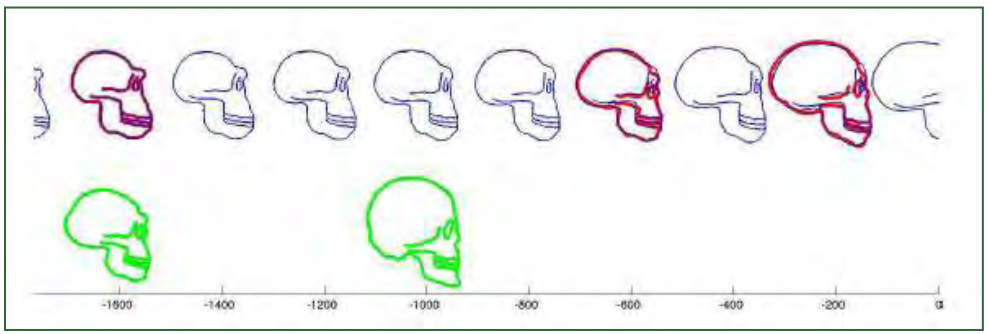

(Homo habilis to sapiens vs. homo erectus)

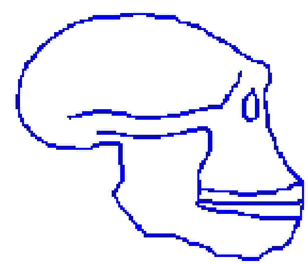

Spatiotemporal variability analysis of longitudinal shape data, S. Durrleman, X. Pennec, A. Trouvé, G. Gerig, N. Ayache

Time warp of 3D shapes

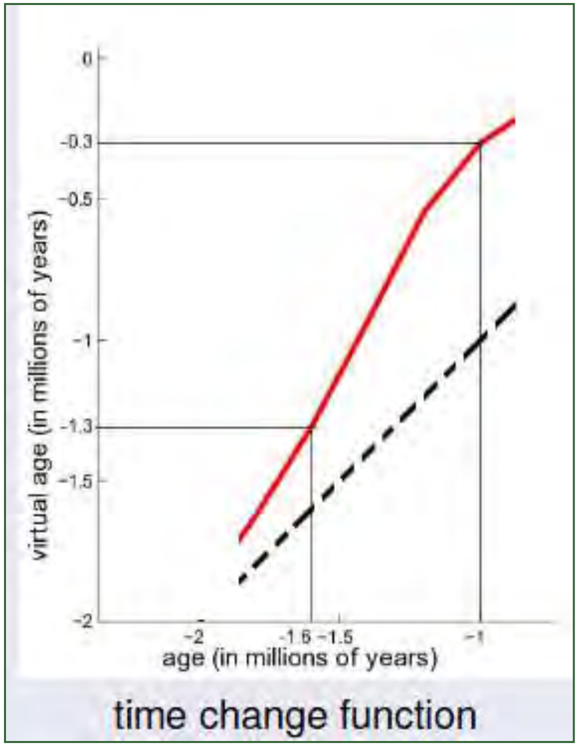

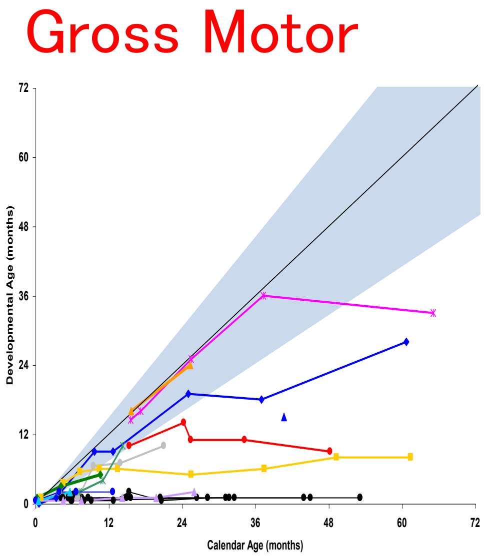

- Captures notion of growth and speed trajectory
- Reflects notion of calendar age versus physiological age
- Scalar model extended to 3D shapes

Preliminary Results: Amygdala Growth in Autism

- 2 scans:
  - initial: age 2-3 years
  - follow-up: age 4-5 years
- 12 subjects:
  - 4 autistics
  - 4 developmental delay
  - 4 controls

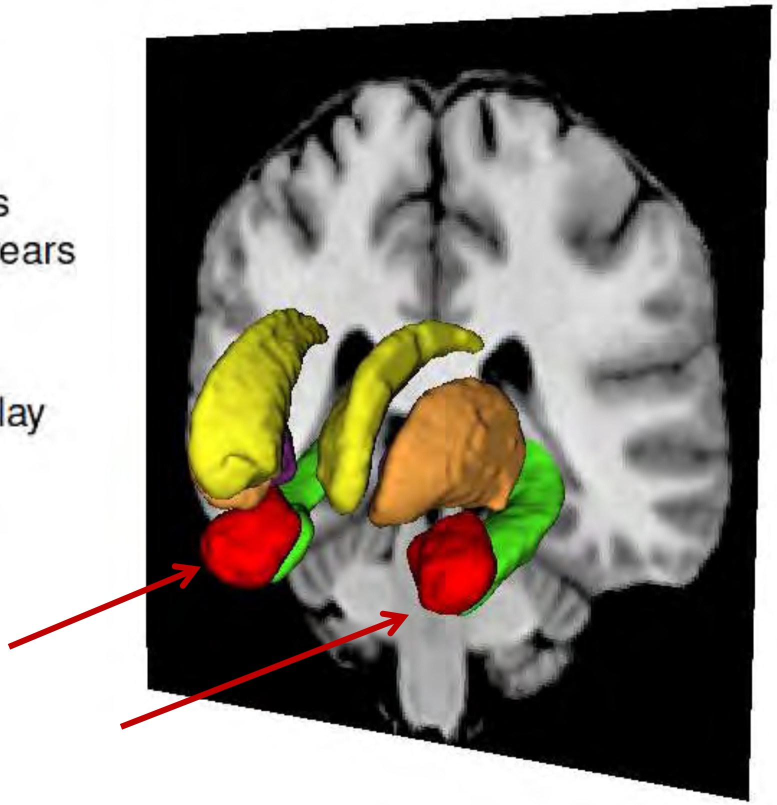

Results: Amygdala Growth in Autism

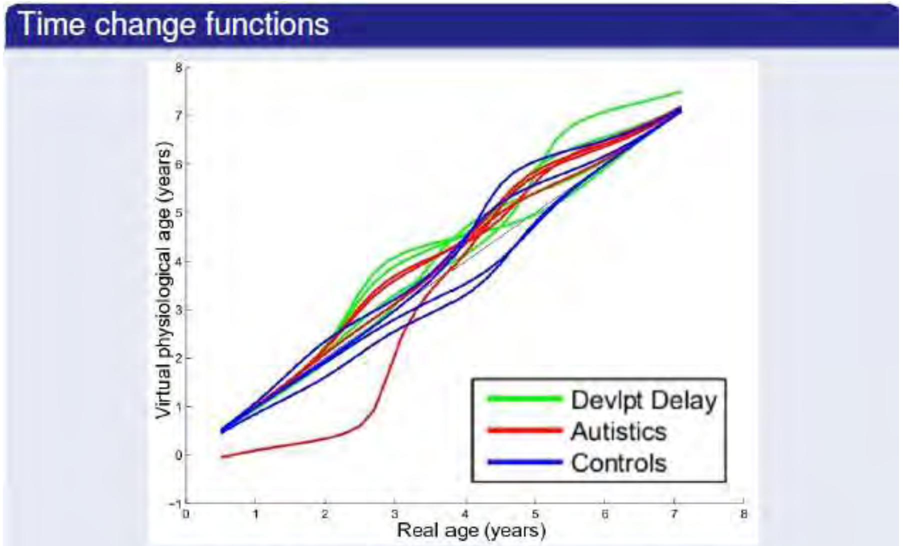

Time change functions (12 raw curves)

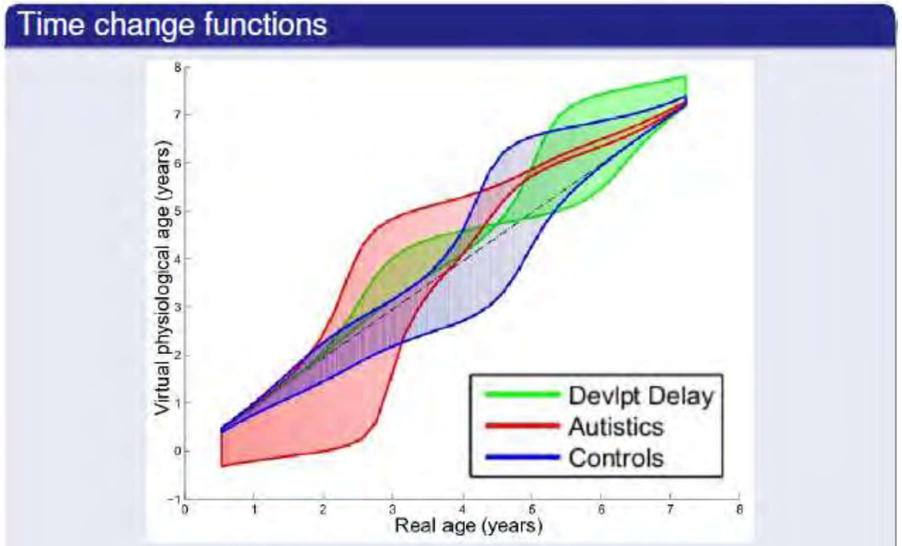

First mode of variations (at $\pm\sigma$)

Conclusions

- Spatio-temporal Image & Shape Analysis: Emerging field with new fundamental problems (math, stats, imaging, modeling):
  - Multidisciplinary by definition.
  - Actively developing field driven by new imaging technologies and novel biomedical driving problems.
  - Challenging fundamental, algorithmic and statistical problems.
  - Research progress enables new scientific discoveries.
- Main driving motivation: Trajectory of change vs. Cross-sectional comparisons.
- Clinically highly relevant: We get 4D longitudinal image data $\rightarrow$ we need powerful tools for quantitative analysis.

Acknowledgements

- **NIH-NINDS**: 1 U01 NS082086-01: 4D Shape Analysis
- **NIH-NIBIB**: 2U54EB005149-06 , NA-MIC: National Alliance for MIC
- **NIH (NICHD) 2 R01 HD055741-06**: ACE-IBIS (Autism Center)
- **NIH NIBIB 1R01EB014346-01**: ITK-SNAP
- **NIH NINDS R01 HD067731-01A1**: Down's Syndrome
- **NIH P01 DA022446-011:** Neurobiological Consequences of Cocaine Use

- **USTAR**: The Utah Science Technology and Research initiative at the Univ. of Utah
- **UofU SCI Institute**: Imaging Research Team
- **Insight Toolkit ITK**

Acknowledgements

Methodology Development:

- James Fishbaugh, Utah
- Marcel Prastawa, ex-Utah (new GE)
- Stanley Durrleman, INRIA Paris
- Xavier Pennec, INRIA Sophia Antipolis

Clinical Longitudinal Imaging:

- Joseph Piven, UNC Psychiatry
- Jane Paulsen and Hans Johnson, U of Iowa
- Lucia Cevidanes, UMICH

Freely available Software

ExoshapeAccel: C/C++ NAMIC toolkit SW for estimating continuous evolution from a discrete collection of shapes,
James Fishbaugh Public download

Stanley Durrleman
http://www.deformetrica.org/

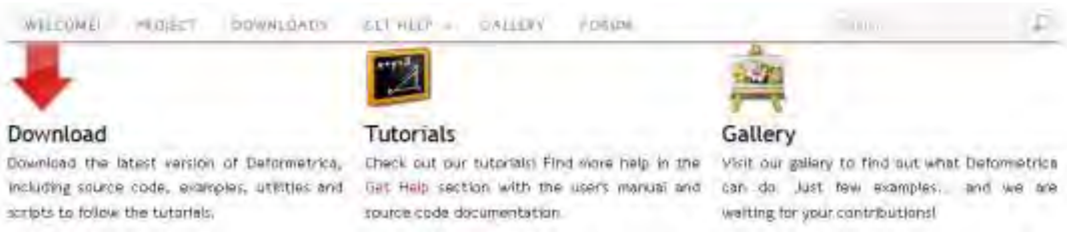

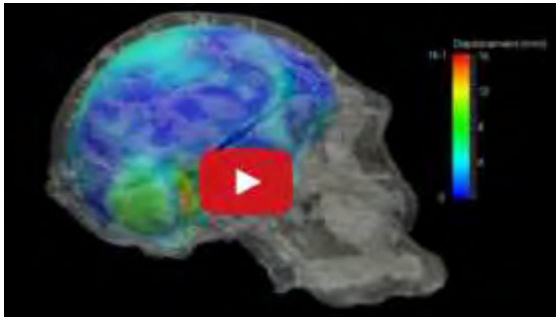

STIA'14 Spatio−Temporal Image Analysis for Longitudinal and Time−Series Image Data

Home

3rd International MICCAI Workshop on Spatiotemporal Image Analysis for Longitudinal and Time-Series Image Data (STIA'14)

MICCAI Workshop Th-W22, Thursday September 18, 2014, Boston

Organizers:

- Guido Gerig, University of Utah, USA (gerig@sci.utah.edu)
- Stanley Durrleman, INRIA, Paris, France (stanley.durrleman@inria.fr)
- Tom Fletcher, University of Utah, USA (fletcher@sci.utah.edu)
- Marc Niethammer, University of North Carolina at Chapel Hill, USA (mn@cs.unc.edu)
- Xavier Pennec, INRIA Sophia Antipolis, France (Xavier.Pennec@sophia.inria.fr)

Sponsors

www.sci.utah.edu

ICM
institut du Cerveau
et de la Moelle épinière

Workshop Proceedings: STIA'14 LNCS Series Springer Verlag